

# Biogeomorphic modeling to assess resilience of tidal marsh restoration to sea level rise and sediment supply

Olivier Gourgue<sup>1,2</sup>, Jim van Belzen<sup>3,1</sup>, Christian Schwarz<sup>4,5</sup>, Wouter Vandenbruwaene<sup>6</sup>, Joris Vanlede<sup>6</sup>, Jean-Philippe Belliard<sup>1</sup>, Sergio Fagherazzi<sup>2</sup>, Tjeerd J. Bouma<sup>3</sup>, Johan van de Koppel<sup>3,7</sup>, Stijn 5 Temmerman<sup>1</sup>

<sup>1</sup> ECOSPHERE Research Group, University of Antwerp, Antwerp, Belgium

<sup>2</sup> Department of Earth and Environment, Boston University, Boston, MA, United States of America

<sup>3</sup> Department of Estuarine and Delta Systems, NIOZ Royal Netherlands Institute for Sea Research, Yerseke, The Netherlands

<sup>4</sup> Department of Civil Engineering, Faculty of Engineering Science, KU Leuven, Leuven, Belgium

10 <sup>5</sup> Division of Geography and Tourism, Department of Earth and Environmental Sciences, KU Leuven, Leuven, Belgium

<sup>6</sup> Flanders Hydraulics Research, Antwerp, Belgium

<sup>7</sup> Conservation Ecology Group, Groningen Institute for Evolutionary Life Sciences, University of Groningen, Groningen, The Netherlands

*Correspondence to:* Olivier Gourgue (ogourgue@gmail.com)

15 **Abstract.** There is an increasing demand for creation and restoration of tidal marshes around the world, as they provide highly valued ecosystem services. Yet, restored tidal marshes are strongly vulnerable to factors such as sea level rise and declining sediment supply. How fast the restored ecosystem develops, how resilient it is to sea level rise, and how this can be steered by restoration design, are key questions that are typically challenging to assess due to complex biogeomorphic feedback processes involved. In this paper, we apply a biogeomorphic model to a specific tidal marsh restoration project 20 planned by dike breaching. Our modeling approach integrates tidal hydrodynamics, sediment transport, and vegetation dynamics, accounting for relevant fine-scale flow-vegetation interactions (less than 1 m<sup>2</sup>) and their impact on vegetation and landform development at the landscape scale (several km<sup>2</sup>) and on the long term (several decades). Our model performance is positively evaluated against observations of vegetation and geomorphic development in adjacent tidal marshes. Model scenarios demonstrate that the restored tidal marsh can keep pace with realistic rates of sea level rise and that its resilience is 25 more sensitive to the availability of suspended sediments than to the rate of sea level rise. We further demonstrate that restoration design options can steer marsh resilience, as they affect the rates and spatial patterns of biogeomorphic development. By varying the width of two dike breaches, which serve as tidal inlets to the restored marsh, we show that a larger difference in the width of the two inlets leads to higher biogeomorphic diversity in restored habitats. This study 30 showcases that biogeomorphic modeling can support management choices in restoration design to optimize tidal marsh development towards sustainable restoration goals.

## 1 Introduction

Tidal marshes are among the most productive ecosystems on Earth (Barbier et al., 2011) providing invaluable services such as protection of coastal settlements against storms (Gedan et al., 2011; Zhu et al. 2020), carbon sequestration (Rogers et al., 2019), maintenance of fisheries (Boesch and Turner, 1984) and water purification (Breaux et al., 1995). They are however

35 among the most threatened ecosystems globally (Barbier et al., 2011). Over centuries, humans have built dikes to prevent tidal flooding and drained soils to gain land for agricultural, industrial, and urban expansion (Gedan et al., 2009). While human-induced degradation and loss have accelerated in recent decades (Deegan et al., 2012; Wang et al., 2014; Tian et al., 2016), remaining tidal marshes are facing the additional global threat of accelerated sea level rise (SLR) caused by climate change (Spencer et al., 2016; Schuerch et al., 2018). In addition, the capacity of tidal marshes to adapt to SLR by sediment 40 accretion and surface elevation gain can be compromised by decreasing sediment supply, for example due to upstream river damming and erosion control measures (Weston, 2014; Yang et al., 2020). Hence, efforts for conservation and restoration of tidal marshes are increasing throughout the world (Mossman et al., 2012; Liu et al., 2016; Zhao et al., 2016; Waltham et al., 2021) with usually the primary goal to support and rehabilitate biodiversity (Armitage et al., 2007; Weinstein, 2007) and provide nursery habitat for commercially important fish and invertebrate species (Rozas and Minello, 2001). Furthermore, 45 marsh restoration is increasingly motivated by its role for nature-based shoreline protection, as marshes attenuate waves, currents and erosion and promote sediment accretion with SLR (Kirwan and Megonigal, 2013; Temmerman et al., 2013; Barbier, 2014; Kirwan et al., 2016; Zhu et al., 2020) and for nature-based mitigation of climate change impacts through carbon sequestration (Barbier et al., 2011; Rogers et al., 2019). The success of restoration designs largely depends on the resulting rates of marsh vegetation development and sediment accretion, as they control the timescales at which target 50 habitats, effective shoreline protection and carbon sequestration are reached. Besides, restoration designs must enable the development of marsh ecosystems that are resilient to modern threats such as SLR and decreasing sediment supply. Yet, predicting actual rates of vegetation development and sediment accretion in establishing marshes, at timescales ranging from years to decades, remains to this day an important challenge (Fagherazzi et al., 2012; Mossman et al., 2012; Wiberg et al., 2020; Fagherazzi et al., 2020; Törnqvist et al., 2021).

55 Managed realignment, which consists in shifting the line of coastal defense structures landward of their existing position, can create space for tidal marsh restoration or creation. This practice has grown in popularity over the last two decades (French, 2006; Turner et al., 2007), especially in the context of coastal squeeze and landward movement of the mean low water mark due to SLR and storms (Doody, 2013). Practically, a second line of defense is built landwards, while the first one is breached. The number and size of breaches are important design choices (Hood, 2014, 2015) and vary greatly between 60 projects (e.g., Friess et al., 2014; Dale et al., 2017). As breaches become the inlets of the restored marshes, they have an important control on water and sediment volumes entering and leaving the system during each tidal cycle, and hence on sediment accretion rates (Oosterlee et al., 2020). Other important design measures may involve excavating an initial channel network and treating soil conditions to facilitate soil drainage (O'Brien and Zedler, 2006), planting manually vegetation

tussocks to ensure vegetation encroachment (Staver et al., 2020), or building hydraulic structures to control the tidal range  
65 and create optimal ecological conditions for vegetation development (Maris et al., 2007; Oosterlee et al., 2018). These design  
choices are mainly driven by restoration objectives and local environmental conditions. Yet, there is high uncertainty in how  
restored tidal marshes develop. For example, several studies point at many restored sites that, in comparison with natural  
tidal marshes, underperform in terms of biodiversity (Wolters et al., 2005; Mossman et al., 2012), topographic diversity  
70 (Lawrence et al., 2018), groundwater dynamics (Tempest et al., 2015; Van Putte et al., 2020) and biogeochemical  
functioning, including carbon sequestration (Santín et al., 2009; Suir et al., 2019). These outcomes can potentially hamper  
marsh ecosystem functions and the initial restoration objectives.

The rate at which tidal marshes develop in restoration projects is highly uncertain, yet so important. For example, sediment  
accretion rates determine whether restored tidal marshes can keep pace with local rates of SLR (Kirwan et al., 2010;  
Vandenbruwaene et al., 2011a; Webb et al., 2013; Kirwan et al., 2016). The establishment rate of pioneer vegetation and the  
75 succession towards climax vegetation may depend on small windows of opportunity that are very difficult to predict  
(Chambers et al., 2003; Hu et al., 2015; Cao et al., 2018). Furthermore, the rate of development is at the center of the tension  
between public perception and restoration objectives. The public opinion is often very critical towards marsh restoration by  
managed realignment, as it implies the loss of valuable land, laboriously reclaimed by previous generations (Temmerman et  
al., 2013). On the one hand, fast development allows to quickly reach target habitats, which may support a positive public  
80 perception, but involves the risk of fast development towards a monotone climax ecosystem state. On the other hand, slow  
development (e.g., including bare mudflats) increases the risk of negative public perception in the first years, but may lead to  
long-term persistence of high habitat diversity with different stages of succession. All these examples illustrate the need for  
modeling tools that are based on state-of-the-art scientific knowledge, and that allow to predict how fast restored tidal  
marshes develop and how development rates can be steered by restoration design.

85 Numerical models of tidal marsh development need to be able to simulate vegetation and landform evolution through  
feedbacks between hydrodynamics, sediment transport and vegetation dynamics. For example, sediment accretion rates  
determine where and when the critical elevation, above which vegetation can grow in the intertidal zone, is reached  
(Bertness and Ellison, 1987; Balke et al., 2016; Bouma et al., 2016). The encroachment of vegetation in turn enhances  
sediment accretion through tidal flow deceleration, direct sediment trapping and organic matter accumulation  
90 (Vandenbruwaene et al., 2011b; Baustian et al., 2012; Fagherazzi et al., 2012). Sediment accretion processes are intrinsically  
linked to the availability of sediments at the marsh edge (Weston, 2014; Liu et al., 2021), as well as their tidal distribution  
along complex channel networks and towards the vegetated platforms (Marani et al., 2003; Temmerman et al., 2005). At the  
same time, vegetation is known to control the morphology of channel networks and their efficiency to deliver sediments into  
the marsh interior (Kearney and Fagherazzi, 2016; Schwarz et al., 2018). So far, spatially explicit models that combine  
95 detailed hydro-morphodynamics with complex vegetation dynamics remain uncommon and their applicability is limited to  
relatively small domains (order of 1 km<sup>2</sup> or less) in comparison to real-life restoration projects of several km<sup>2</sup> (Temmerman  
et al., 2007; Best et al., 2018; Schwarz et al., 2018; Bij de Vaate et al., 2020; Wang et al., 2021). In contrast, there are

relatively fewer applications on large-scale domains (several km<sup>2</sup> or more) and these applications usually rely on relatively coarse grid resolutions (order of 100 m – e.g., Mariotti and Canestrelli, 2017), short simulation periods (order of 1 decade – 100 e.g., Brückner et al., 2019), simplified hydro-morphodynamics (Craft et al., 2009; Alizad et al., 2016; Spencer et al., 2016; Mariotti, 2020; Mariotti et al., 2020) or simplified vegetation dynamics (D’Alpaos et al., 2007; Belliard et al., 2015). One of the great challenges in numerical modeling of tidal marsh development is to combine large domains (order of 1 km<sup>2</sup> or more), fine grid resolution (order of 1 m<sup>2</sup> or less) and stochasticity in pioneer vegetation establishment, which are all essential to capture relevant scale-dependent biogeomorphic feedbacks, such as flow concentration between small-scale 105 pioneer vegetation patches (order of m<sup>2</sup> – van Wesenbeeck et al., 2008; Gourgue et al., 2021) and its impact on the landscape-scale formation of channel networks (order of km<sup>2</sup> – Temmerman et al. 2007; Schwarz et al. 2018). To date, this full range of scales in biogeomorphic feedbacks has never been included in a single numerical model for long-term tidal marsh development (from several decades to a century).

In this paper, we present a biogeomorphic model application to a specific tidal marsh restoration project by managed 110 realignment, accounting for relevant fine-scale flow-vegetation interactions (less than 1 m<sup>2</sup>) and their impact on vegetation and landform developments at the landscape scale (several km<sup>2</sup>). The novelty of this paper is threefold. First, we evaluate the long-term resilience (several decades) of a large-scale restored tidal marsh project (several km<sup>2</sup>) in response to different rates of SLR and different concentrations of suspended sediment supply. Second, we investigate how that resilience can be affected by restoration design options (here, the inlet configuration). Third, we evaluate our model performance against data 115 on vegetation and geomorphic development in adjacent tidal marshes.

## 2 Methods

### 2.1 Multiscale biogeomorphic modeling

We have developed the biogeomorphic modeling framework Demeter to simulate explicitly, in an intertidal landscape, the 120 feedbacks between (i) tidal hydrodynamics, (ii) sediment erosion, transport, deposition, and resulting bed level changes, and (iii) vegetation establishment, expansion and die-off for multiple dominant vegetation types. We adopt a multiscale approach (Fig. 1a), in which the hydro-morphodynamics is computed at a grid resolution of 5 m, while the vegetation dynamics is computed at a much finer grid resolution of 25 cm. This multigrid approach enables to reduce the uncertainty arising from heterogeneous small-scale processes such as stochastic vegetation establishment (Temmerman et al., 2007; Schwarz et al., 2018) and plant-flow-sediment interactions around vegetation patches (van Wesenbeeck et al., 2008; Schwarz et al., 2015). It 125 however requires the development of specific multiscale coupling techniques to preserve subgrid-scale heterogeneity while information is exchanged between the two modules (Gourgue et al., 2021). In this section, we describe the general principles of our modeling approach. See Sect. S1 (supplementary material) for more details.

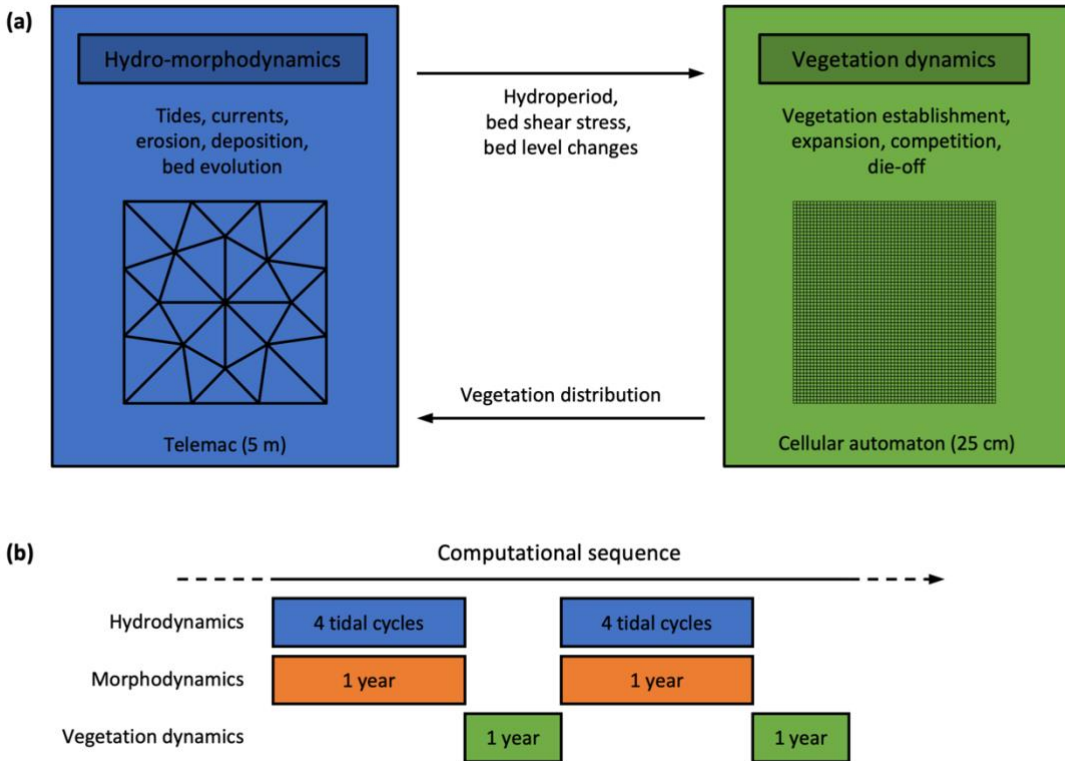


**Figure 1: Schematic representation of the multiscale biogeomorphic coupling. (a)** Telemac is used for the hydro-morphodynamics at relatively coarse resolution (5 m) and a cellular automaton is used for the vegetation dynamics at finer resolution (25 cm). **(b)** Hydrodynamics and morphodynamics are constantly coupled (every time step). The morphological acceleration method allows to upscale four semi-diurnal tidal cycles of hydrodynamics into one year of morphodynamic evolution. Hydro-morphodynamics and vegetation dynamics are coupled once a year.

### 2.1.1 Hydro-morphodynamic module

Demeter is in principle compatible with any process-based hydro-morphodynamic model. Here we use the finite element solver suite Telemac (version 7.3.0), more specifically its modules Telemac-2D for hydrodynamics and Sisyphe for sediment transport and morphodynamics. Telemac-2D simulates water level fluctuations and flow velocities by solving the depth-averaged shallow water equations in a two-dimensional horizontal framework (Hervouet, 2007). The vegetation resistance force is modeled as the drag force on a random array of potentially submerged rigid cylinders with uniform properties per species (Baptist et al., 2007) and calibrated against flume measurements (Vandenbruwaene et al., 2011b; Bouma et al., 2013; Gourgue et al., 2021). Sisyphe simulates the transport of cohesive sediments by solving the depth-averaged advection-diffusion equation, as well as bed level changes through sediment erosion (Partheniades, 1965) and deposition (Einstein and Krone, 1962).

### 2.1.2 Vegetation module

145 Demeter includes a cellular automaton that is used here for the vegetation dynamics. A cellular automaton consists of a regular grid of cells, each one with a finite number of states (here, vegetation species). Cells can change their state in discrete time steps, depending on their neighborhood state and a set of simple stochastic transition rules (Balzter et al., 1998). The cellular automaton simulates here the fate of three generic species representative of pioneer, middle marsh and high marsh plants encountered nearby the study site. Transition rules (i.e., for vegetation establishment, lateral expansion, species competition and vegetation die-off) are determined based on field observations and depend on environmental stressors 150 provided by Telemac (i.e., hydroperiod, bed shear stress and bed level changes).

Based on observations in the vicinity of the study site, expected vegetation species that are representative for pioneer, middle marsh and high marsh vegetation are, respectively, *Aster tripolium*, *Scirpus maritimus* and *Phragmites australis*. In the model, the different species establish within different hydroperiod ranges. Within their hydroperiod range, *Aster tripolium* 155 has a relatively high probability of establishment, but no possibility to expand laterally in patches, while *Scirpus maritimus* and *Phragmites australis* have relatively low probabilities of establishment, but their vegetated grid cells can expand laterally and form patches that grow at rates of several  $\text{m yr}^{-1}$ . For each species, vegetated grid cells can potentially die if the bed shear stress or the erosion is too high. See Sect. S1.6 (supplementary material) for more details.

### 2.1.3 Biogeomorphic coupling

160 During one sequence of hydro-morphodynamics, Telemac keeps track of different environmental stressors (i.e., hydroperiod, bed shear stress and bed level changes), which are then used to regulate the transition rules for vegetation establishment, lateral expansion, species competition and vegetation die-off in the vegetation module. During one sequence of the vegetation module, the cellular automaton updates the distribution of vegetation, which is then used to evaluate the vegetation resistance force in the hydro-morphodynamic module. See Sect. S1.3 and S1.4 (supplementary material) for more 165 details.

### 2.1.4 Computation sequence

The computation sequence is schematized in Fig. 1b. We use the morphological acceleration method to decouple hydrodynamic and morphodynamic timescales (Lesser et al., 2004; Roelvink, 2006). The hydrodynamics is computed with time steps of 1.5 s. At every time step of the hydro-morphodynamic model, bed level changes are multiplied by the 170 morphological acceleration factor  $\alpha$ , so that after simulating one semi-diurnal tidal cycle (12h25'), we have in fact extrapolated morphological changes to cover  $\alpha$  cycles. The originality of our method is that we have selected four different semi-diurnal tidal cycles (that is, one neap, one spring and two intermediate cycles, with high-water level intervals ranging from 0.3 to 0.5 m) from a larger, estuarine-scale hydrodynamic model. Each tidal cycle is considered representative of a class of tides with similar high tide levels (as computed from data records over 10 years in a station nearby the study site)

175 and is assigned with a different value of  $\alpha$ , which is determined proportionally to the relative number of tides in its own class. The sum of all  $\alpha$  values is determined so that the four representative tidal cycles correspond to one year of morphological changes. After one year of hydro-morphodynamics, the cellular automaton simulates one year of vegetation dynamics based on yearly aggregated information from the hydro-morphodynamic model (i.e., hydroperiod, bed shear stress and bed level changes). The updated spatial vegetation distribution is finally passed to the hydro-morphodynamic model, and  
180 as such the procedure is repeated to produce calculations of hydro-morphodynamics and vegetation dynamics for the next year. To mimic the effect of SLR, the bottom elevation is lowered every year by a value corresponding to the yearly increase of mean sea level (MSL). All simulations in this paper are for a period of 50 years.

## 2.2 Study site: managed realignment of Hedwige-Prosper Polder

Hedwige-Prosper Polder (Fig. 2) is an agricultural area of 4.65 km<sup>2</sup> situated at the Belgian/Dutch border along the Scheldt  
185 Estuary. The surrounding region has a long embankment history, starting from the Middle Ages, including large scale intentional dike breaching for military operations in the late 16<sup>th</sup> century, and followed by subsequent stepwise re-embankment projects until the early 20<sup>th</sup> century (Jongepier et al., 2015). In the coming years, the dikes of Hedwige Polder on the Dutch side (2.95 km<sup>2</sup>) and Prosper Polder on the Belgian side (1.70 km<sup>2</sup>) will be breached to re-introduce tides and  
190 restore natural intertidal habitats (Boerema et al., 2016). This managed realignment project is part of the Sigma Plan, which aims at improving flood protection in the tidal part of the Scheldt basin in Belgium (Smolders et al., 2015), while at the same time restoring natural estuarine habitat (Cox et al., 2006; Maris et al., 2007). Here, the tidal marsh restoration project consists of building a new ring dike at the landward side of the area (Fig. 2c, green line) and removing parts of the old dike (Fig. 2c, red line) to allow daily tidal inundation and spontaneous development of an intertidal ecosystem. To facilitate the drainage of  
195 the area right from the start, the restoration design also includes the excavation of an initial channel network (Fig. 2c, blue line) and part of the fringing marshes and mudflats at the seaward side of the old dike (Fig. 2c, purple line). The excavated material is used to raise the landscape in Prosper Polder to partially compensate its lower elevation (Fig. 2c, yellow area) and create breeding islands for birds (Fig. 2c, pink areas). By design, the restored tidal marsh will be a multi-inlet system, with a larger inlet in Hedwige Polder (further referred to as the Northern basin) and a smaller inlet in Prosper Polder (further referred to as the Southern basin). The restored area also includes the existing marsh of Sieperdaschor (Fig. 2c – further  
200 referred to as the old marsh). Right before de-embankment, the mean platform elevation with respect to the local mean high-water level (MHWL) will be -1.14 m in the Northern basin and -1.24 m in the Southern basin.

Local environmental conditions are determinant for the development of restored ecosystems (Liu et al., 2021). The Scheldt  
Estuary, here defined as the tidal part of the Scheldt River, is a semidiurnal macrotidal estuary extending over 160 km. At a  
205 gauge station near Bath (Fig. 2b), the tidal range has been recorded to vary on average from 4.21 m at neap tides to 5.76 m at spring tides during the period 2011-2015, and the MHWL to rise at a rate of 5.7 mm yr<sup>-1</sup> during the period 1931-2004 (Wang and Temmerman, 2013). This MHWL rise rate is used here as proxy for SLR rate (Sect. 2.3). The study site lies in the brackish zone of the estuary, which is characterized by a steep gradient in salinity, with values ranging from 5 to 18 PSU

(Van Damme et al., 2005; Meire et al., 2005). Therefore, only a limited number of vegetation species (Sect. 2.1) can cope with the local environmental conditions. The local SSC is influenced by the presence of a maximum turbidity zone, where  
210 large volumes of cohesive sediments are concentrated and continually resuspended by the tidal flow (Baeyens et al., 1997; Chen et al., 2005; Meire et al., 2005). At the study site, the current average SSC is estimated at  $63 \text{ mg l}^{-1}$  (Sect. S2, supplementary material). Sediment accretion in marshes of the Scheldt Estuary is dominated by the external supply by tides of suspended sediments, mostly of mineral nature, while organic matter only accounts for about 10% of the measured  
215 accretion rates (Temmerman et al., 2004). For this reason, our model does not explicitly simulate organic matter accretion locally produced by vegetation.

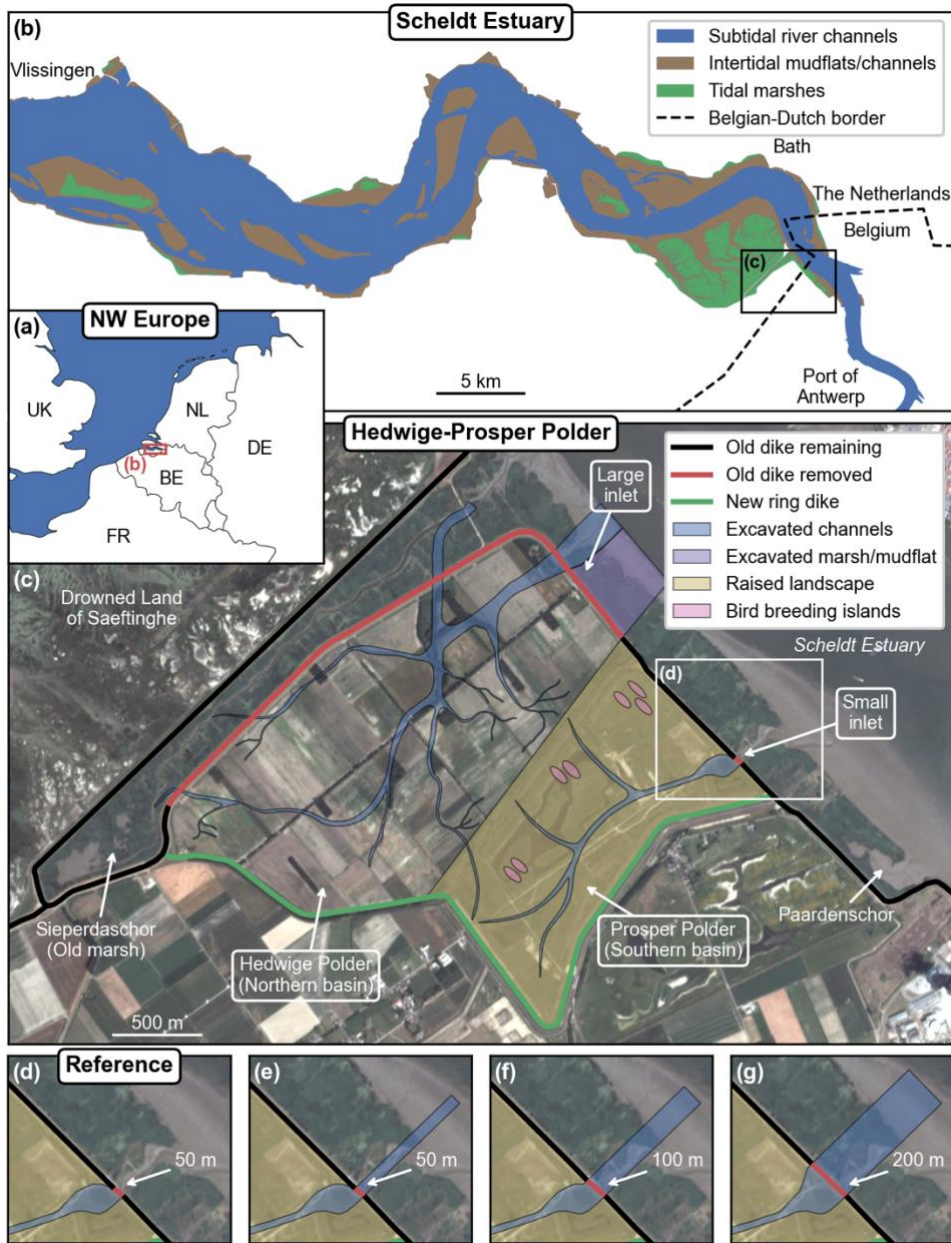


**Figure 2: Overview of the study site location within Northwestern Europe (a) and along the Scheldt estuary (b). Overview of the managed realignment project design (c) with close-up views of the small inlet according to the reference design (d) and three alternative designs (e-g), which consist of different breach sizes and the excavation of a straight channel between the dike breach and the main estuarine subtidal channel. The satellite image is a PlanetScope 4-band multispectral orthorectified scene (Planet Team, 2017) from July 4, 2019. The restoration design data are provided by the Vlaams-Nederlandse Scheldecommissie (VNSC). Other spatial data are from Natural Earth, Rijkswaterstaat, OpenStreetMap and EuroGeographics. © OpenStreetMap contributors 2020. Distributed under the Open Data Commons Open Database License (ODbL) v1.0.**

### 2.3.1 Sea level rise rate and suspended sediment concentration

We investigate the resilience of the restored tidal marsh to human-induced climate and environmental changes by considering different relative SLR rates and different SSC at the seaward boundary (Table 1). If our model can account for changes in MSL (Sect. 2.1), changes in MHWL are more relevant for the biogeomorphology of tidal marshes, as the 230 intertidal elevation relative to MHWL determines the tidal inundation regime, hence affecting sediment accretion rates (Temmerman et al., 2004) and vegetation growth (Balke et al., 2016). Therefore, for the reference model scenario, we consider a SLR rate corresponding to the average rate of MHWL rise observed in the Scheldt Estuary over the last century, that is,  $6 \text{ mm yr}^{-1}$  (Temmerman et al., 2004; Wang and Temmerman, 2013). This relatively high rate of MHWL rise is partly due to global SLR but also likely amplified by local human-induced changes in the geomorphology of the estuary, such as 235 historical embankment of intertidal areas and widening and deepening of the navigation channels (Smolders et al., 2015; Wang et al., 2019). We also consider two additional scenarios, with no ( $0 \text{ mm yr}^{-1}$ ) and high ( $12 \text{ mm yr}^{-1}$ ) SLR rate, respectively. In comparison, SLR rate projections for the period 2005-2055 at the estuary mouth range between 4.8 and 6.3 mm/yr (median projections for Representative Concentration Pathways 2.6 and 8.5 – IPCC, 2019). With these relatively extreme additional scenarios, we can therefore reasonably assume that we cover the range of possible future SLR rates in the 240 area.

Human activities can also potentially disturb the estuarine sediment dynamics. For example, river damming and erosion control measures in the upstream river catchment can potentially reduce the sediment supply to the estuary (Svitski et al., 2009; Yang et al., 2020), while increasing tidal intrusion can potentially increase the SSC (Winterwerp et al., 2013). As sediment supply is critical for marsh development (Hopkinson et al., 2018; Liu et al., 2021), we consider three scenarios with 245 different SSC at the seaward boundary, that is, the reference scenario with an SSC of  $63 \text{ mg l}^{-1}$ , as observed nearby the study site (Sect. S2, supplementary material), as well as two additional scenarios with low ( $30 \text{ mg l}^{-1}$ ) and high ( $120 \text{ mg l}^{-1}$ ) SSC, respectively.

### 2.3.2 Small-inlet design

We also investigate the impact of restoration design on the rates of spatial vegetation and landform development. In 250 particular, the width of the dike breaches (i.e., the inlets of the restored marsh) is an important design choice in managed realignment projects. Here, we simulate four different versions of the small inlet (Fig. 2d-g, Table 1). We first consider the reference design (Fig. 2d), which simply consists of a 50-meter-wide breach in the old dike. We then explore three alternative designs with respectively a 50-, 100- and 200-meter breach, along with the excavation of a straight channel of the same width between the dike breach and the main estuarine subtidal channel (Fig. 2e-g).

255 **2.3.3 Vegetation dynamics**

In the reference model scenario, vegetation establishes randomly following different colonization strategies (i.e., either homogeneously with relatively high probability of establishment but no possibility to expand laterally, or patchily with relatively low probability of establishment but possibility to expand laterally to form growing patches – Sect. S1.2, supplementary material) in areas where environmental stressors allow for it (Sect. 2.1.2). This is the expected behavior  
260 supported by field observations for the three selected species representative for pioneer, middle and high marsh vegetation (Sect. S1.5.2, supplementary material). To illustrate the impact of the vegetation dynamics on the biogeomorphic feedbacks and the model results, we also consider six variants of the reference model scenario (Table S1).

**Table 1: Model scenarios.**

Model scenario	Sea level rise rate	Suspended sediment concentration	Small inlet design		
			Breach width	Excavated channel	Figure
#1 (reference)	6 mm yr <sup>-1</sup>	63 mg l <sup>-1</sup>	50 m	No	Figure 2d
#2	0 mm yr <sup>-1</sup>	63 mg l <sup>-1</sup>	50 m	No	Figure 2d
#3	12 mm yr <sup>-1</sup>	63 mg l <sup>-1</sup>	50 m	No	Figure 2d
#4	6 mm yr <sup>-1</sup>	30 mg l <sup>-1</sup>	50 m	No	Figure 2d
#5	6 mm yr <sup>-1</sup>	120 mg l <sup>-1</sup>	50 m	No	Figure 2d
#6	6 mm yr <sup>-1</sup>	63 mg l <sup>-1</sup>	50 m	Yes	Figure 2e
#7	6 mm yr <sup>-1</sup>	63 mg l <sup>-1</sup>	100 m	Yes	Figure 2f
#8	6 mm yr <sup>-1</sup>	63 mg l <sup>-1</sup>	200 m	Yes	Figure 2g

**2.4 Evaluation of model performance**

265 We have developed a model to predict the biogeomorphic evolution of a restored tidal marsh in an area that is still embanked. Due to lack of in situ data to validate our modeling approach, we evaluate its overall performance against observations in nearby intertidal mudflats and marshes. This is done for the reference model scenario (Sect. 2.3 and Table 1). Observations on elevation change (Sect. 2.4.1) and vegetation development (Sect. 2.4.2) are used for qualitative model calibration, based on model sensitivity to a selection of sediment parameters (i.e., critical shear stress for erosion, settling  
270 velocity, dry bulk density and incoming SSC) and vegetation parameters (i.e., establishment probability and patch expansion

rate). Observations on channel network characteristics (Sect. 2.4.3) are used for qualitative model validation. In some cases, we calculate linear regressions from both model results and observations, and we perform an analysis of covariance (ANCOVA) to determine whether they are significantly different from each other (Sect. 2.4.4).

#### **2.4.1 Sediment accretion on vegetated platforms**

275 Sediment accretion processes on vegetated platforms are crucial for marsh resilience against SLR (Kirwan et al., 2016). Based on digital elevation maps derived from historical topographic surveys in the adjacent marshes of the Drowned Land of Saeftinghe (Fig. 2c) between 1931 and 1963 (Wang and Temmerman, 2013), we have developed an empirical relationship between mean elevation change on vegetated platforms and mean high-water depth. Here, we develop a similar relationship based on model results in the restored tidal marsh, using the same variables over the same time interval (i.e., between years 280 18 and 50 after de-embankment), and we compare it with the empirical relationship derived from observations. See Sect. S2 (supplementary material) for more details.

#### **2.4.2 Pioneer vegetation development**

285 The encroachment of vegetation on intertidal platforms impacts sedimentation in tidal marshes, and hence their geomorphic development (Mudd et al., 2010). Here, we compare our model results with observed rate of spatial expansion of the vegetation cover in the adjacent restored marshes of Paardenschor (Fig. 2c), from its de-embankment in 2004 until 2017. See Sect. S3 (supplementary material) for more details.

#### **2.4.3 Channel geometric properties**

290 Channel networks control the flow of water and sediments in tidal marshes, and their evolution interact with the biogeomorphic development of the surrounding intertidal platforms (D'Alpaos et al., 2007; Kearney and Fagherazzi, 2016). Here, we compare various geometric properties of the simulated tidal channels with observations in the adjacent marshes of the Drowned Land of Saeftinghe (Fig. 2c – Vandenbruwaene et al., 2013, 2015). To that end, we have developed a quasi-automatic methodology to extract tidal channel networks and related geometric properties from model results. More 295 specifically, we compute the probability distribution of unchanneled flow length (i.e., the shortest distance to a channel bank) as a measure of channel density (Tucker et al., 2001). The mean unchanneled flow length is calculated as the slope of the linear portion of the probability distribution when plotted on semi-log axes (Marani et al., 2003; Chirol et al., 2018). Along the channel network skeleton (i.e., the channel centerlines – Fagherazzi et al., 1999), we compute the watershed area, the upstream mainstream channel length (i.e., the longest upstream channel within the watershed), the mean overmarsh tidal prism (i.e., the mean high-tide water volume within the watershed for all tides overtopping the surrounding platform – Vandenbruwaene et al., 2013, 2015) and the channel cross-sectional dimensions (i.e., channel width, channel depth and 300 channel cross-section area). We also verify the applicability of Hack's law, an empirical power relationship that links watershed area and mainstream channel length (Rigon et al., 1996). See Sect. S4 (supplementary material) for more details.

#### 2.4.4 Linear regressions and analysis of covariance

In several cases, we calculate linear regressions from both model results and observations. First, w2e split the data into 10 sub-samples of equal size, based on the x-axis variable (i.e., the first sub-sample includes the 10% smallest values, etc.).

305 Then, we calculate the mean value of each sub-sample, and we derive the linear regressions from these mean values. Finally, we perform an ANCOVA to determine whether linear regressions from model results and observations are significantly different from each other. Two null hypotheses are tested. The first null hypothesis is that the slopes of the regression lines are equal, and the second that their intercepts are equal. For each of these two tests, we calculate the associated p-value. Two regression lines are significantly different from each other if at least one p-value is lower than 0.05. If both p-values are 310 higher than 0.05, the regression lines are statistically equal.

#### 2.5 Vertical datums and metrics used for result analysis

Elevation data are either expressed with reference to the Normaal Amsterdams Peil (NAP), the official vertical datum in the Netherlands, which represents approximately the MSL at the Dutch coast, or the local MHWL.

315 The mean platform elevation over a certain area (i.e., the Northern basin, the Southern basin, or both combined) is calculated excluding channels and supratidal areas (i.e., the highest parts of the dikes and constructed bird breeding islands). The vegetation cover over a certain area is calculated as the proportion of vegetated cells, excluding supratidal areas.

The ebbing time is a proxy for the drainage efficiency of an inlet and is calculated as the time needed to drain 95% of the total ebb volume. The ebb volume is the instantaneous volume of water flowing through an inlet since high tide during the ebb phase (i.e., from high to low tide in the estuary). The total ebb volume is the ebb volume at the end of the ebb phase (i.e., 320 at low tide). The relative ebb volume is the instantaneous ebb volume divided by the total ebb volume.

### 3 Results

#### 3.1 Reference model scenario

The results of the reference model scenario indicate that the system is predominantly depositional (Fig. 3f-j), with only localized erosion up to about 10 cm yr<sup>-1</sup> concentrated near the inlets and in some initially excavated channels in the first ten 325 years (Fig. 3f) and in some newly formed channels afterwards (Fig. 3g-j). In general, the development of vegetation (Fig. 3k-o) follows the topographic evolution (Fig. 3a-e), as higher elevations decrease hydroperiods and increase establishment chances. Replicate simulations of the reference model scenario indicate that stochasticity in vegetation development influences where secondary channels form.

In the first 10 to 20 years, most sedimentation occurs in the back of the Northern basin and almost everywhere in the 330 Southern basin (Fig. 3a-b and Fig. 3f-g), where pioneer vegetation and then middle marsh vegetation start to encroach whenever the elevation, and hence the hydroperiod, becomes suitable (Fig. 3k-l). The middle marsh vegetation ability to

colonize its surroundings via clonal expansion (Sect. 2.1) is especially visible in years 20 and 30 (Fig. 3l-m). In general, middle marsh and high marsh vegetation follow similar colonization strategies, but with a 10- to 20-year delay (Fig. 3l-o).

In the first 20 to 30 years, some of the initially excavated channels are predicted to fill up (Fig. 3f-h) or even to disappear over time (Fig. 3c-e), especially those oriented perpendicular to the tidal flow propagation. Meanwhile, newly formed channels are primarily created by differential deposition (Fig. 3g-h), although erosion starts to occur in a second phase when they become narrower (Fig. 3h-j). In general, vegetation does not encroach in tidal channels before they fill up, because the hydroperiod and the shear stress are too high.

Overall, the presence of vegetation has a positive impact on platform accretion rates in the Northern basin, although the speed of colonization has nearly no influence on the mean platform elevation 50 years after de-embankment (Fig. S1a, supplementary material). In the Southern basin, neither the presence of vegetation nor the speed of colonization seems to affect sediment accretion on the platforms (Fig. S1b, supplementary material), which suggests that the hydrodynamics is predominant in that part of the restored marsh. Locally, the vegetation dynamics can have remarkable geomorphic effects, such as the maintenance or disappearance of pre-excavated channels, whether we consider no vegetation, the reference vegetation dynamics, or instantaneous colonization (Fig. S2). In general, vegetation input parameters have a rather limited impact on the long-term morphodynamics (Fig. S3).

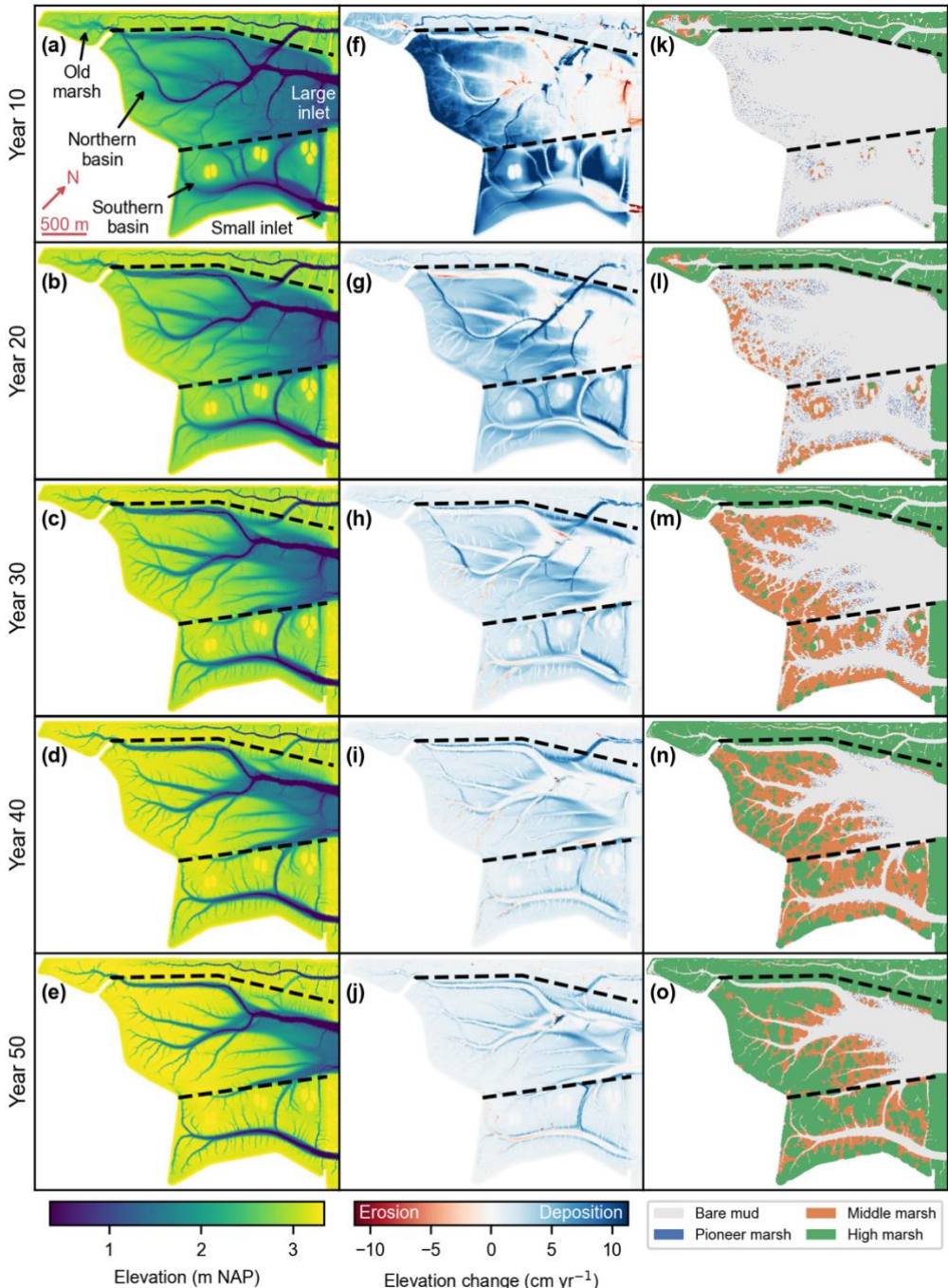
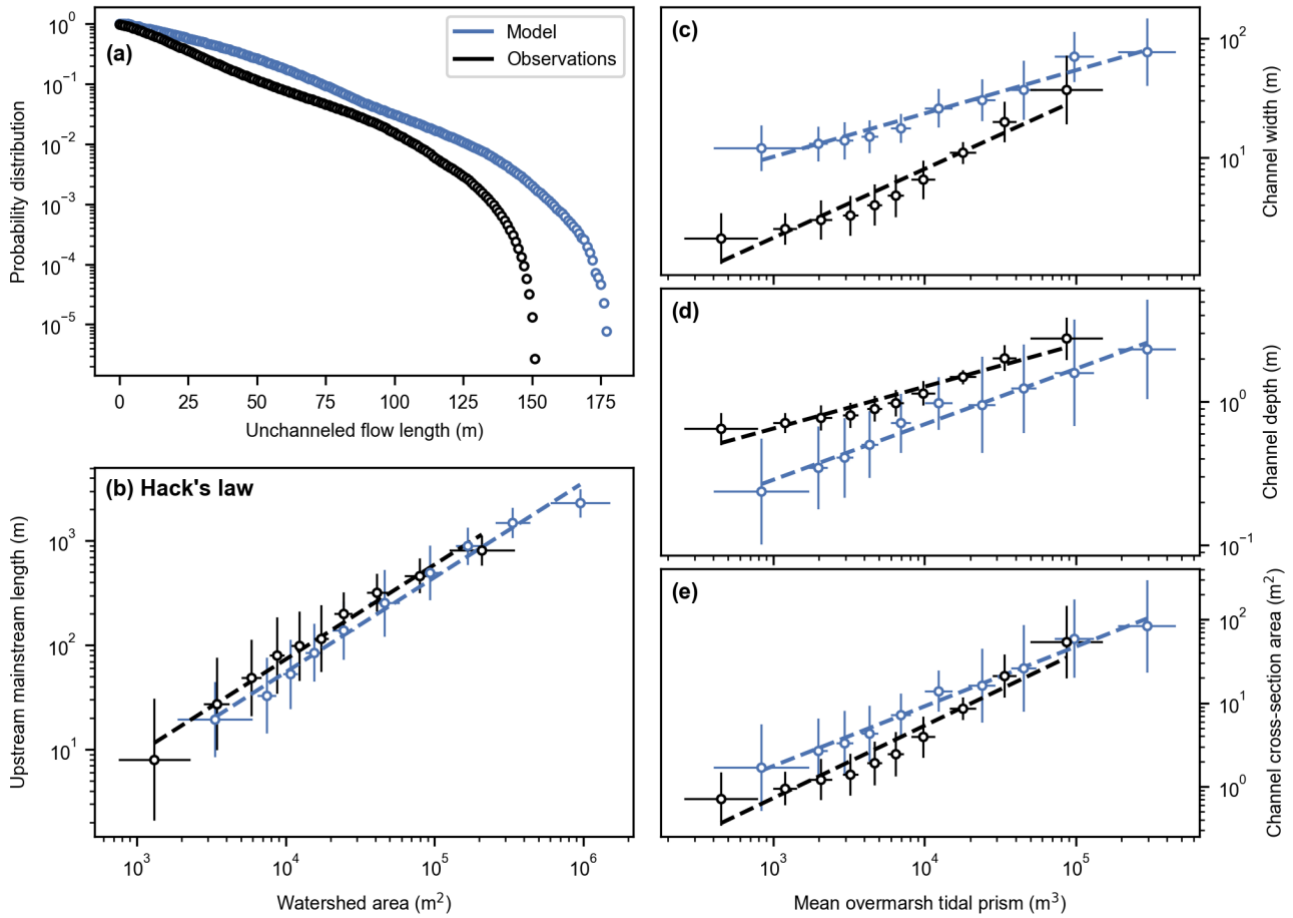


Figure 3: Reference model scenario (#1). Bed elevation (a-e), bed elevation change (f-j) and vegetation distribution (k-o) every 10 years after de-embankment. The bed elevation change is calculated as the mean difference over the previous 10 years. The dashed lines delineate the old marsh, the Northern basin, and the Southern basin. All figures are rotated by 43° clockwise, as compared to Fig. 2c.

### 3.2 Evaluation of model performance

Our results for the reference model scenario are in good agreement with the empirical relationship between mean elevation  
355 change on vegetated platforms and mean high-water depth, which is obtained from observations in a tidal marsh close to the study site (Fig. S4, supplementary material). The linear regressions obtained from model results and observations are statistically equal, as both their slopes ( $p = 0.496$ ) and their intercepts ( $p = 0.412$ ) are not significantly different (Table S2, supplementary material). This suggests that sediment accretion processes on vegetated platforms are well represented in our model. Predicted vegetation cover development is also in good agreement with observations in another restored tidal marsh  
360 close to the study site (Fig. S5, supplementary material).

The predicted channel network 50 years after de-embankment is slightly less dense, as compared with observations in a nearby tidal marsh (Fig. 4a), with mean unchannelled flow lengths of respectively 26.0 m (model) and 23.7 m (observations). The exponent of Hack's law is 0.908 for the model results and 0.909 for the observations (Fig. 4b). These values are statistically equal as the slopes of the linear regressions are not significantly different ( $p = 0.913$  – Table S2, supplementary material). However, their intercepts are significantly different ( $p = 0.007$ ), which means that the predicted channel lengths are smaller than those observed in the nearby natural marsh, with regards to the local watershed area. The exponent of the power law in Fig. 4e is 0.71 for the model results and 0.87 for the observations. These values are not statistically equal as the slopes of the linear regressions are slightly, but significantly different ( $p = 0.023$ ). The intercepts are also significantly different ( $p = 0.004$ ), which means that predicted channel cross-section areas are larger than those observed in the nearby  
365 tidal marsh, with regards to the local tidal prism. The relatively important deviations between model results and observations in terms of channel width and channel depth (Fig. 4c-d and Table S2, supplementary material) partly compensate each other, so that the discrepancy in channel cross-section area is much smaller, but also decreases with increasing tidal prism (Fig. 4e).  
370



**Figure 4: Reference model scenario (#1). Channel geometric properties 50 years after de-embankment (blue) compared to observations in an established marsh close to the study site (black). Probability distribution of the unchanneled flow length (a), upstream mainstream length vs. watershed area (b), and channel width (c), channel depth (d) and channel cross-section area (e) vs. mean overmarsh tidal prism. (b-e) Model results and observations are respectively split into 10 sub-samples of equal size (Sect. 2.4.4). Markers and error bars represent the geometric means and standard deviations of each sub-sample, respectively. Dashed lines represent geometric regressions of the geometric means.**

375

### 380 3.3 Impact of sea level rise and sediment supply

Our results indicate that the restored tidal marsh is resilient to realistic ranges of SLR rate and SSC at the seaward boundary (Fig. 5). Indeed, for every model scenario considered, the intertidal platforms accrete faster than SLR (Fig. 5a-b) and the restored area can sustain a growing vegetation cover (Fig. 5c-d).

385

In Fig. 5a-b, we show the mean platform elevation with respect to MHWL, which increases over time due to SLR, rather than a fixed level like NAP. This is especially relevant when comparing the system response to different SLR rate scenarios. In terms of absolute platform elevation (i.e., with respect to a fixed level like NAP), increasing rates of SLR leads to faster platform accretions. However, the rate at which intertidal platforms catch up with MHWL decreases with increasing rates of

SLR (Fig. 5a). This is especially relevant in terms of marsh resilience, which is defined as the ability to keep pace with SLR. Platform elevation (Fig. 5a-b) is also related to vegetation development (Fig. 5c-d), which is driven by hydroperiod rather  
390 than absolute elevation. That is why we choose to present the mean platform elevation with respect to the MHWL.

By the end of the 50-year simulated period, the system has not reached an equilibrium, where both mean platform elevation and vegetation cover converge to a stable value. Nevertheless, it can be extrapolated from our results that equilibrium will occur slower for increasing rate of SLR (Fig. 5a, c) and decreasing sediment supply (Fig. 5b, d). Interestingly, within the range of considered parameter values, the rate of biogeomorphic development seems more sensitive to suspended sediment  
395 availability (Fig. 5b, d) than SLR rate (Fig. 5a, c).

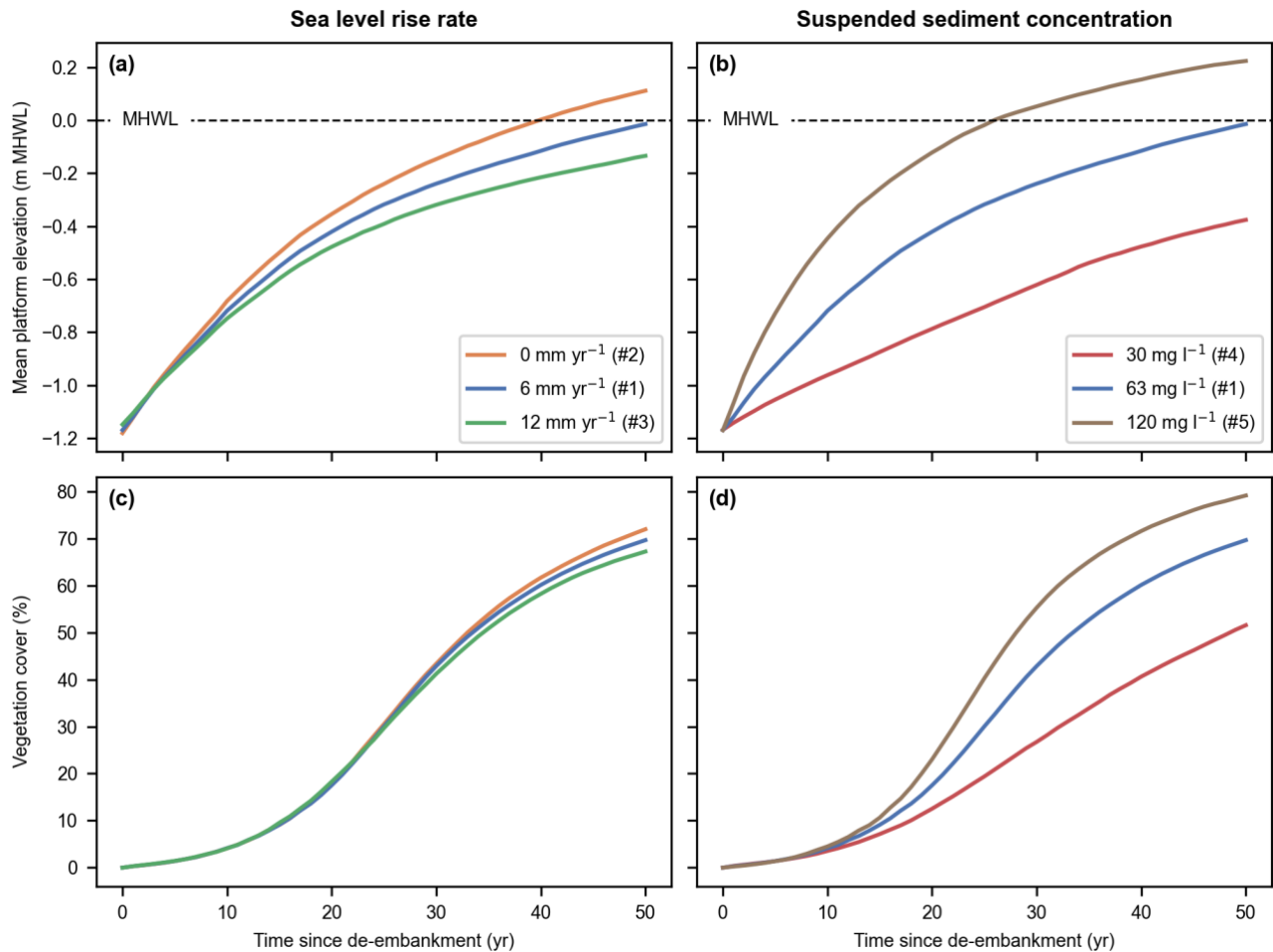


**Figure 5: Sea level rise rate (a, c) and suspended sediment concentration (b, d) model scenarios (#1-5). Evolution of the mean platform elevation with respect to the mean high-water level (MHWL) (a-b) and development of the vegetation cover (c-d) in the Northern and Southern basins combined.**

400 3.4 Impact of inlet width

To investigate the impact of inlet width, we first analyze separately how the large-inlet Northern basin and the small-inlet Southern basin (Fig. 2c) behave for the reference scenario. We then compare model scenarios with increasing inlet widths in the Southern basin.

Our results indicate that, for the reference design, the Southern basin develops faster than the Northern basin (Fig. 6a-b).

405 During the flood phase (Fig. 7a-c), water and suspended sediments fill the Southern basin through the small inlet, but also from the Northern basin. Conversely, in the first part of the ebb phase (Fig. 7d-e), water and suspended sediments leave the Southern basin both through the small inlet and towards the Northern basin. However, in the second part of the ebb phase (Fig. 7f), the water surface elevation in the Southern basin drops below the Northern basin platforms, so that water and suspended sediments can only flow towards the small inlet. Meanwhile, the small inlet slows down the evacuation of the 410 remaining water, giving more time to suspended sediments to settle in the Southern basin.

This interpretation is confirmed by an analysis of the water volume and sediment mass budgets during a spring tide in the first year after de-embankment (Fig. 8). At the boundary between the Northern and Southern basins, there is 40% more water entering the Northern basin during the flood phase than leaving it during the ebb phase (Fig. 8a, pink). Consequently, the small-inlet ebb discharge is 40% higher than its flood discharge (Fig. 8a, blue). Besides, it takes 40 more minutes to flush the 415 water through the small inlet than through the large inlet (Fig. 6c), which gives 30% more time for suspended sediments to settle in the Southern basin after high tide. This leads to 60% more sedimentation in the Southern basin than in the Northern basin (Fig. 8b, black). The same pattern can be observed, albeit to a lesser degree, for intermediate and neap tides, as well as at later stages of marsh development.

Our argument that faster biogeomorphic development in the Southern basin is due to enhanced sediment trapping related to 420 its small inlet size is further supported by the three alternative design scenarios (Fig. 2e-g). Our results indeed demonstrate that widening the small inlet slows down the biogeomorphic development in the Southern basin (Fig. 9b, d). It has however the opposite effect in the Northern basin, where widening the small inlet leads to faster biogeomorphic development (Fig. 9a, c). At the landscape scale, widening the small inlet leads to the formation of more, larger channels that originate from the 425 small inlet and expand into the Northern basin (Fig. 10, ellipses). This contributes to the supply of more sediments into the Northern basin. Interestingly, while the width of the small inlet clearly affects the spatial distribution of sedimentation and vegetation development in the restored marsh, it barely impacts the general biogeomorphic trend when the Northern and Southern basins are considered combined (Fig. S6, supplementary material). Overall, it is a zero-sum game where the Northern and Southern basins act like communicating vessels.

The ebbing time remains very close to an average value of 3h08' (standard deviation of 2') for both inlets and all designs

430 (Fig. 9e-f), except in the case of the small inlet in its reference design (3h54').

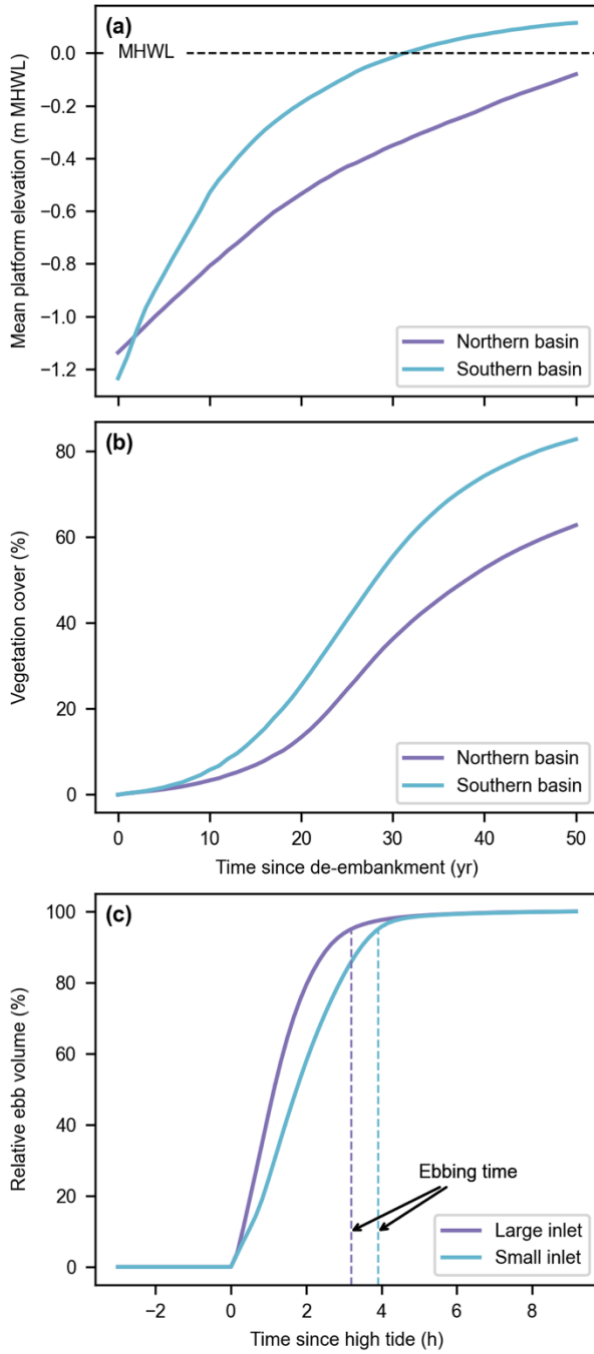
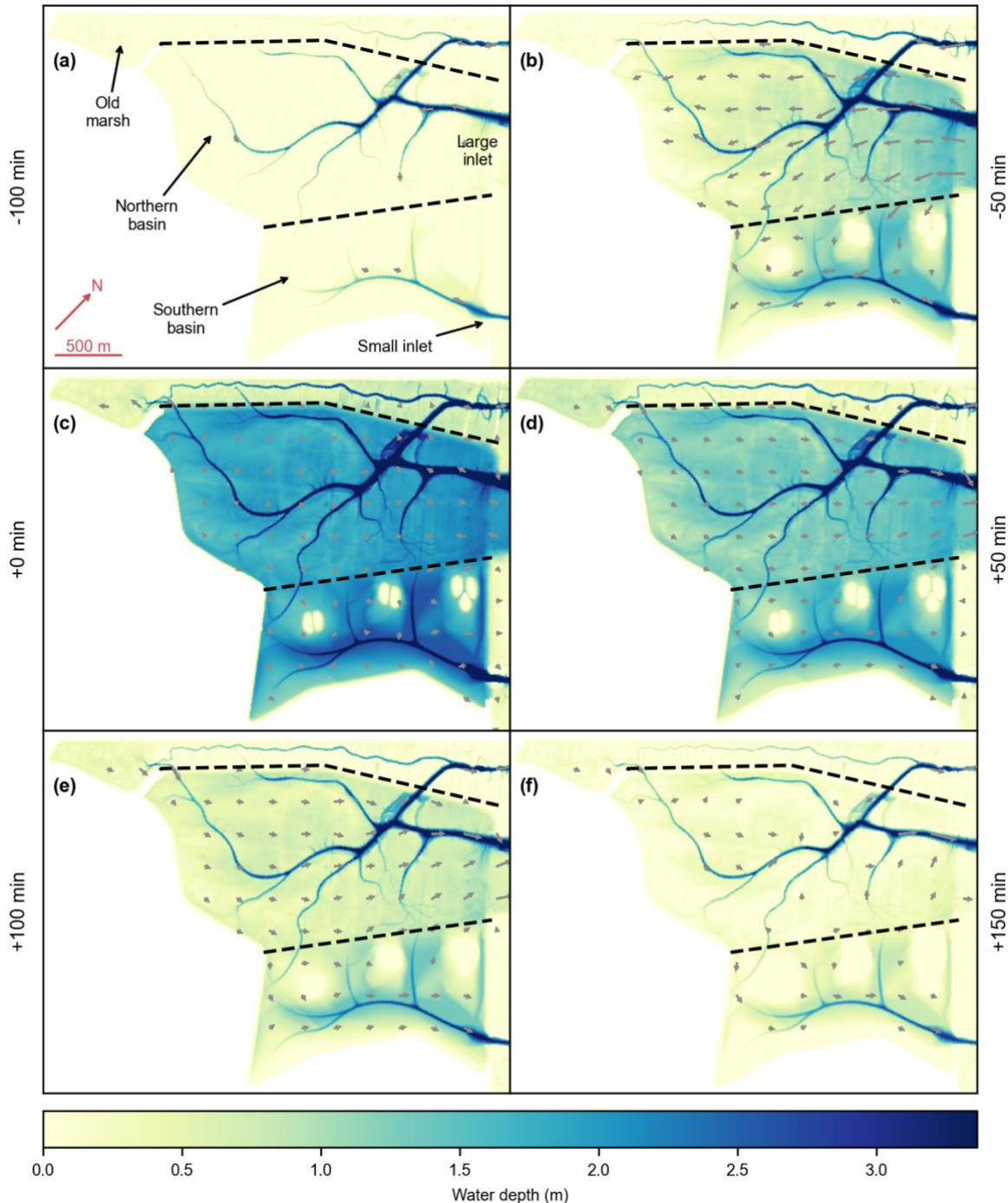
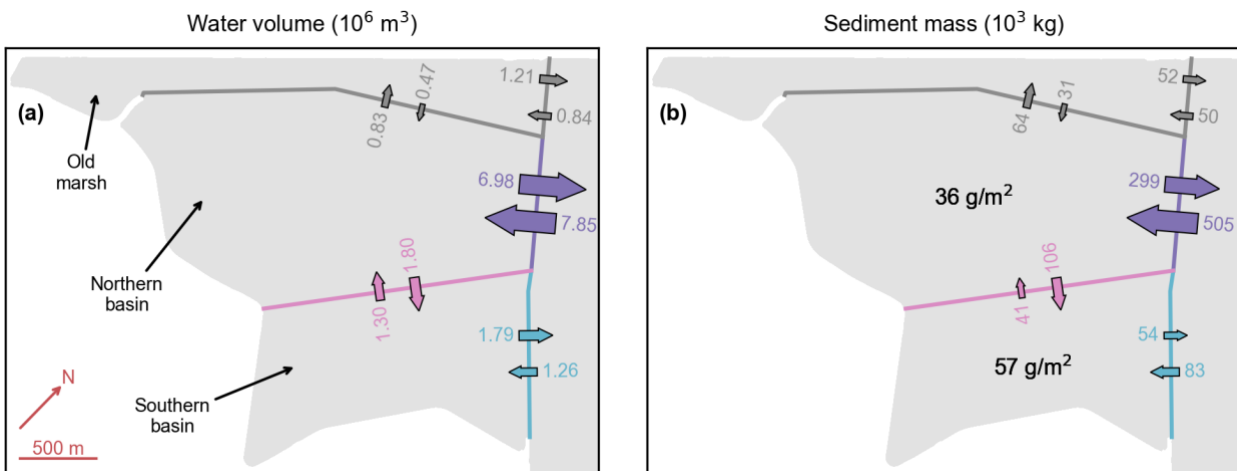


Figure 6: Reference model scenario (#1). Evolution of the mean platform elevation with respect to the mean high-water level (MHWL) (a) and development of the vegetation cover (b) in the Northern and Southern basins. Evolution of the relative ebb volume (i.e., the percentage of water volume flowing through an inlet since high tide during the ebb phase, see Sect. 2.5) and resulting ebbing time (i.e., the time corresponding to a relative ebb volume of 95%, proxy for inlet flush efficiency, see Sect. 2.5) for the large and small inlets during a spring tide of the first year after de-embankment (c).



**Figure 7: Reference model scenario (#1).** Water depth (color maps) and flow velocity (grey arrows) every 50 minutes during a spring tide of the first year after de-embankment. Time tags are relative to high tide. Flow velocity arrows are not displayed if their magnitude is lower than  $0.1 \text{ m s}^{-1}$  or if the water depth is lower than 10 cm. The dashed lines delineate the old marsh, the Northern basin, and the Southern basin. All figures are rotated by  $43^\circ$  clockwise, as compared to Fig. 2c.



**Figure 8: Reference model scenario (#1). Water volume (a) and sediment mass (b) budgets during a spring tide in the first year after de-embankment. Color numbers and arrows represent water volumes and sediment masses flowing into and away from the different basins. Black numbers represent the resulting sediment deposition during that period. All figures are rotated by  $43^\circ$  clockwise, as compared to Fig. 2c.**

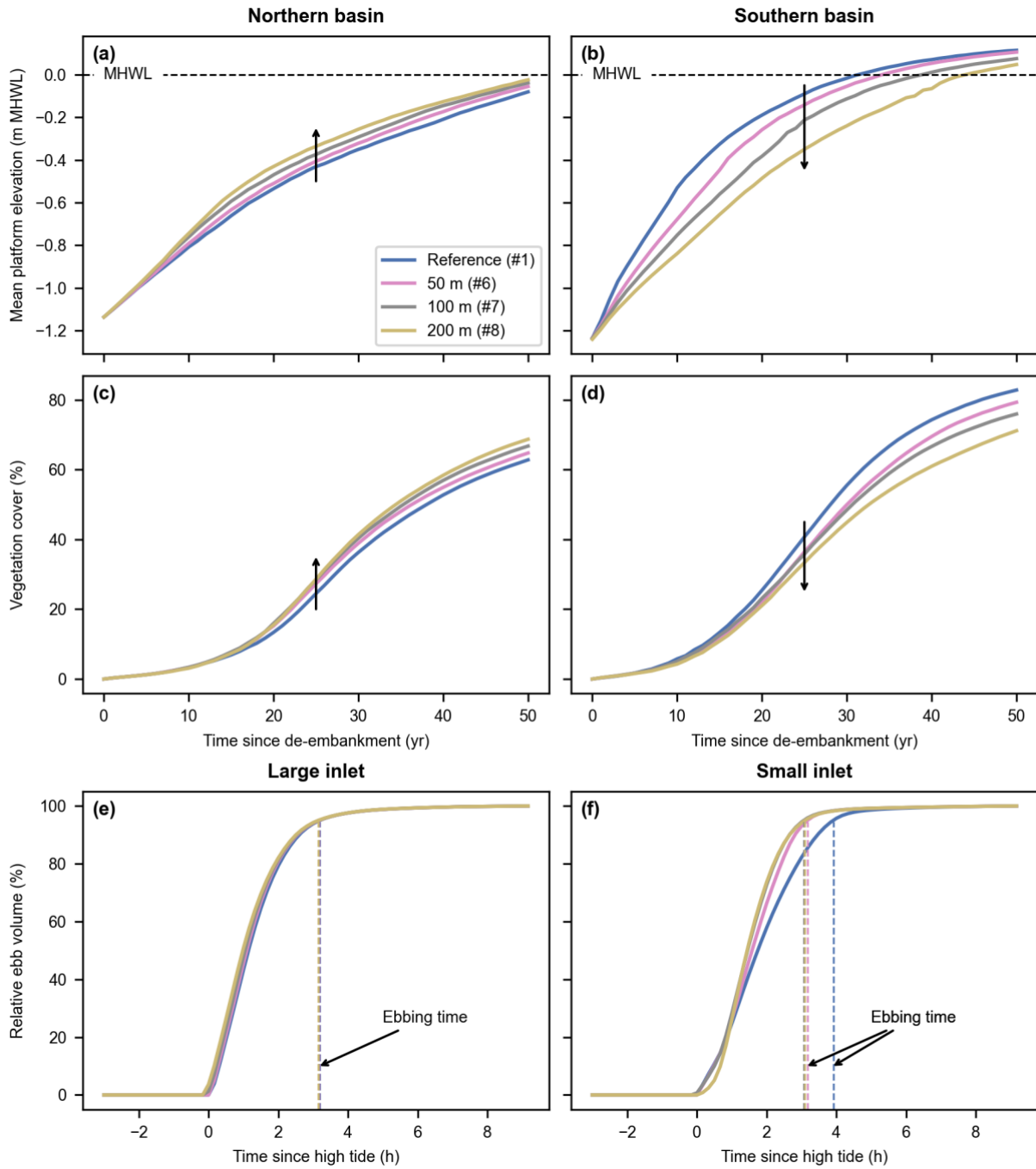
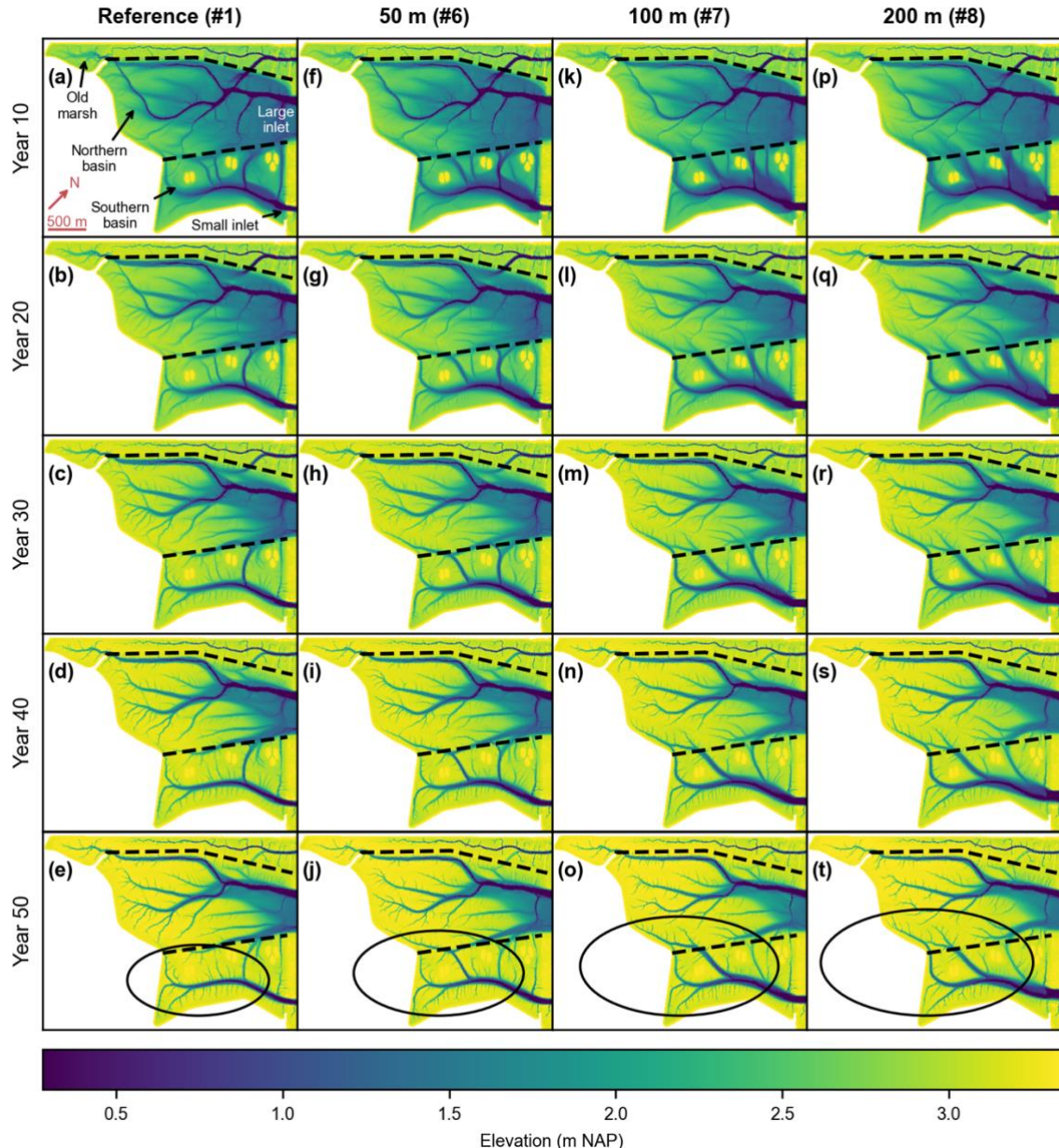


Figure 9: Inlet design model scenarios (i.e., reference design and three alternative designs with small-inlet widths of respectively 50, 100 and 200 m, and an excavated channel – #1, 6-8). Evolution of the mean platform elevation with respect to the mean high-water level (MHWL) (a-b) and development of the vegetation cover (c-d) in the Northern (a, c) and Southern basins (b, d). Evolution of the relative ebb volume (i.e., the percentage of water volume flowing through an inlet since high tide during the ebb phase, see Sect. 2.5) and resulting ebbing time (i.e., the time corresponding to a relative ebb volume of 95%, proxy for inlet flush

efficiency, see Sect. 2.5) for the large (e) and small (f) inlets during a spring tide of the first year after de-embankment. Black arrows highlight trends for increasing small-inlet widths (a-d) or indicate the ebbing time (e-f).



455  
**Figure 10: Inlet design model scenarios (i.e., reference design (a-e) and three alternative designs with small-inlet widths of**  
 460 **respectively 50 m (f-j), 100 m (k-o) and 200 m (p-t), and an excavated channel – #1, 6-8). Bed elevation every 10 years after de-**  
**embankment. The dashed lines delineate the old marsh, the Northern basin, and the Southern basin. The ellipses emphasize the**  
**channel network that originates from the small inlet and its expansion into the Northern basin with increasing small-inlet size. All**  
**figures are rotated by 43° clockwise, as compared to Fig. 2c.**

## 4 Discussions

The increasing demand for creation and restoration of resilient tidal marshes calls for the development of new modeling tools. These models must be able to assess whether rates of biogeomorphic development will achieve restoration objectives, as well as how these rates can be eventually steered by restoration design. In this paper, we present a novel biogeomorphic model application to a tidal marsh restoration project in a macrotidal estuary. We find that the ability of the restored marsh to sustain future rates of SLR is more sensitive to suspended sediment availability than to rates of SLR (Fig. 5). We also demonstrate that inlet design can steer rates and spatial patterns of biogeomorphic development (Fig. 9-10), and as such can be used to achieve specific restoration objectives.

### 4.1 Biogeomorphic modeling as a tool to optimize tidal marsh restoration design

470 One of the main objectives in every tidal marsh restoration project is for intertidal platforms to build vertically faster than SLR, allowing to develop and maintain a vegetation cover. In that context, local environmental conditions play a crucial role. In the case studied here, our model predicts that, for the first 50 years, the restored tidal marsh can keep pace with realistic rates of SLR, and that its resilience is more sensitive to suspended sediment availability (Fig. 5). These findings are in line with previous studies on marsh adaptability to SLR. For example, an ensemble model study indicates that tidal marshes with 475 similar sediment input and tidal range as our study site can cope with SLR rates up to  $70 \text{ mm yr}^{-1}$  in the 21st century (Kirwan et al., 2010, 2016). Here, we test SLR rates up to  $12 \text{ mm yr}^{-1}$  in the first 50 years after de-embankment, for which we predict a highly resilient restored marsh. Furthermore, a recent global assessment of tidal marsh and mangrove restoration projects reveals that the ability of coastal wetlands to keep pace with SLR is mostly driven by suspended sediment availability (Liu et al., 2021), which is also in line with our results.

480 A second key question that is typically raised when planning for tidal marsh restoration is how fast the ecosystem and its different habitat zones develop (Yando et al., 2019), which is for a large part driven by the rates of sediment accretion, pioneer vegetation establishment and succession. Here, the desired rates depend on the restoration objectives. High rates of sediment accretion and vegetation development allow to quickly reach certain restoration objectives, such as different aspects of nature-based shoreline protection. For example, high-lying and densely vegetated marshes are most effective for 485 wave attenuation (Möller, 2006; Schoutens et al., 2020; Willemsen et al., 2020), and reduction of shoreline erosion (Möller et al., 2014; Francalanci et al., 2013; Wang et al., 2017; Schoutens et al., 2019) and dike breaching hazards (Zhu et al., 2020). However, when tidal marshes are created along estuaries or deltas to attenuate extreme high tides and storm surges (Smolders et al., 2015; Stark et al., 2017; Huguet et al., 2018; Smolders et al., 2020), lower accretion rates are preferred to maintain higher water storage capacity in the restored tidal marshes. When the objective is to restore intertidal habitats and 490 meet specific biodiversity goals (Hinkle and Mitsch, 2005; Chang et al., 2016), it may be favorable for accretion rates to be high so that vegetation can develop fast, but also not too fast so that a diversity of habitats can persist over time, including tidal channels, mud flats, pioneer marsh and higher marsh vegetation, while avoiding a rapid succession to climax species. In

the case studied here, our model predicts that the reference restoration design can achieve the objective of intertidal biodiversity rehabilitation. Indeed, because of the relatively slow accretion rates in the Northern basin (Fig. 6), the restored 495 tidal marsh still features the entire range of intertidal habitats after 50 years (Fig. 3).

The examples above illustrate the need to identify restoration design options that can steer rates of sediment accretion and vegetation development in line with restoration objectives. In this study, we focus on the impact of one specific design option: the inlet width (Fig. 2). Our model predicts that, for the setting studied here, higher differences between the two inlet widths lead to more contrasting sedimentation and vegetation patterns in the two basins (Fig. 9). This has two positive 500 outcomes. On the one hand, high accretion rates in the Southern basin bring fast vegetation development there, and potentially positive public perception for the restoration project. On the other hand, lower accretion rates in the Northern basin allow for long-term persistence of habitat diversity, which is an important objective in this project. Other important 505 design options, such as the excavation of a channel network (Williams et al., 2002; Wallace et al., 2005; Hood, 2014), the manual planting of vegetation (O'Brien and Zedler, 2006; Staver et al., 2020), the infilling or lowering of areas, or the creation of a landward slope, were beyond the scope of this study. However, new fundamental insight on the impact of such 510 design options is crucial and should be investigated in the future. Our novel biogeomorphic model is made available for the scientific community in this perspective (see Code and data availability).

## 4.2 Evaluation of model performance

An important challenge for tidal marsh biogeomorphic models is that rates of sediment accretion and vegetation 510 development are highly uncertain (Wolters et al., 2005; French, 2006; Mossman et al., 2012; Spencer and Harvey, 2012). For example, exposure to wind waves and resulting sediment resuspension processes (Leonardi et al., 2016) can considerably 515 lower accretion rates and potentially prevent any vegetation to establish (French et al., 2000). In contrast, improper inlet design can lead to very high accretion rates of poorly consolidated sediments that also limit vegetation establishment (Oosterlee et al., 2020). Other important sources of uncertainty for vegetation development include biotic control such as 520 benthic animals grazing on establishing plants (Paramor and Hughes, 2005; Silliman et al., 2005) and plant stress related to extreme events such as droughts or hurricanes (Howes et al., 2010). At this stage, our model is not equipped to evaluate these uncertainties.

However, to our knowledge, this paper presents the first application of a tidal marsh biogeomorphic model accounting for 520 relevant fine-scale interactions (less than 1 m<sup>2</sup>) between flow and stochastic, patchy vegetation establishment patterns, as well as their long-term impact (several decades) at the landscape scale (several km<sup>2</sup>) on vegetation and landform development. Previous studies were either limited to smaller domains (order of 1 km<sup>2</sup> or less – Temmerman et al., 2007; Best et al., 2018; Schwarz et al., 2018; Bij de Vaate et al., 2020; Wang et al., 2021), coarser grid resolutions (order of 100 m – Mariotti and Canestrelli, 2017), shorter simulation periods (order of 1 decade – Brückner et al., 2019), more simplified hydro-morphodynamics (Craft et al., 2009; Alizad et al., 2016; Spencer et al., 2016; Mariotti, 2020; Mariotti et al., 2020) or 525 more simplified vegetation dynamics (D'Alpaos et al., 2007; Belliard et al., 2015). However, our model does not include

certain processes that are accounted for in other recent marsh models, but that are considered not relevant for this specific study case, such as wind waves (Mariotti and Canestrelli, 2017; Best et al., 2018; Mariotti, 2020) and pond dynamics (Mariotti et al., 2020).

Studies that evaluate the performance of a tidal marsh biogeomorphic model against field observations of marsh development over relevant spatio-temporal scales (several km<sup>2</sup> and decades) are rather scarce. In this paper, we show that our model results are in relatively good agreement with observations from tidal marshes close to the study site, in terms of sediment accretion rates on vegetated platforms (Fig. S4, supplementary material), vegetation cover development (Fig. S5, supplementary material) and channel geometric properties (Fig. 4). The discrepancies between model results and observations in channel width and channel depth, and to a lesser degree in channel cross-section area, may be related to different factors. With a spatial resolution of 5 m, the model is unable to develop channels narrower than 10 to 20 m, while the observations come from remote sensing images with a spatial resolution of 50 cm, revealing channel widths as narrow as a few meters (Fig. 4c). Concomitantly, if the model overestimates the width of channels, this leads to a lower capacity for flow concentration and channel deepening through erosion, which can explain why the model predicts shallower channels, as compared to observations (Fig. 4d). Moreover, observations come from a much older marsh, which was also created by dike breaching of a former polder area, but around 400 years ago (Jongepier et al., 2015). Fifty years after de-embankment, our restored tidal marsh is probably still at an earlier stage of development, as compared to the reference marsh. D'Alpaos et al. (2006) show that the width-to-depth ratio of channels decreases with marsh age. This is line with our model results, which indicate that channel depth increases over time, although channel width remains stable (Fig. S7, supplementary material), probably because of the grid resolution limitations discussed above. Finally, the SSC in the estuary is on average 1.5 times higher in the vicinity of the study site, as compared to the adjacent reference marsh where observations come from (Sect. S2, supplementary material). However, our model results indicate that even reducing the sediment availability by a factor of 2 has nearly no impact on the channel geometric properties (Fig. S8, supplementary material). In any case, discrepancies in channel cross-section area are much smaller, as compared to channel width and channel depth, and they decrease with tidal prism (Fig. 4e).

## 550 5 Conclusions

In this paper, we present a biogeomorphic model application to a specific tidal marsh restoration project by managed realignment at the Belgian/Dutch border along the macrotidal Scheldt Estuary. Our results indicate that the restored tidal marsh can keep pace with realistic rates of SLR and that its resilience is more sensitive to suspended sediment availability, in agreement with current scientific knowledge. Our results further demonstrate that restoration design options can steer the 555 biogeomorphic development of restored tidal marshes, and as such can be used as means to achieve specific restoration objectives.

Predicting the rate of restored tidal marsh development is very important, yet highly uncertain. Our novel biogeomorphic model, whose performance is here evaluated against observations in tidal systems close to the study site, is an attempt to reduce that uncertainty. Our promising results call for the evaluation of additional restoration design options.

## 560 **Code and data availability**

The biogeomorphic model Demeter is available at <https://doi.org/10.5281/zenodo.5205258>. The Python toolbox

TidalGeoPro to compute geometric characteristics of tidal channel networks is available at

<https://doi.org/10.5281/zenodo.5205285>. The multipurpose Python toolbox OGTools is available at

<https://doi.org/10.5281/zenodo.3994952>. The data and source code to reproduce all figures and analyses are available at

565 <https://doi.org/10.5281/zenodo.5898146>.

## **Author contribution**

Conceptualization: OG, JvB, CS, TJB, JvdK, ST. Data curation: OG. Formal analysis: OG, JvB. Funding acquisition: OG, SF, TJB, JvdK, ST. Investigation: OG, JvB. Methodology: OG, JvB, CS, JPB, SF, TJB, JvdK, ST. Project administration: OG, SF, JvdK, ST. Resources: WV, JV. Software: OG. Supervision: SF, TJB, JvdK, ST. Validation: OG. Visualization: OG.

570 Writing – original draft: OG. Writing – review and editing: all co-authors.

## **Competing interests**

The authors declare that they have no conflict of interest.

## **Acknowledgments**

This project has received funding from the Vlaams-Nederlandse Scheldecommissie (VNSC), the European Union's Horizon 575 2020 research and innovation program (Marie Skłodowska-Curie Actions – global postdoctoral fellowship – grant nr. 798222) and the Research Foundation – Flanders (FWO – fundamental research project – grant nr. G060018N). The resources and services used in this work were provided by the VSC (Flemish Supercomputer Center), funded by the Research Foundation – Flanders (FWO) and the Flemish Government. SF was partly funded by the USA National Science Foundation awards 1637630 (PIE LTER) and 1832221 (VCR LTER).

580 **References**

Alizad, K., Hagen, S.C., Morris, J.T., Bacopoulos, P., Bilskie, M.V., Weishampel, J.F., and Medeiros, S.C.: A coupled, two-dimensional hydrodynamic-marsh model with biological feedback, *Ecol. Model.*, 327, 29-43, <https://doi.org/10.1016/j.ecolmodel.2016.01.013>, 2016.

Armitage, A.R., Jensen, S.M., Yoon, J.E., and Ambrose, R.F.: Wintering shorebird assemblages and behavior in restored tidal wetlands in Southern California, *Restor. Ecol.*, 15, 139-148, <https://doi.org/10.1111/j.1526-100x.2006.00198.x>, 2007.

Baeyens, W., van Eck, B., Lambert, C., Wollast, R., and Goeyens, L.: General description of the Scheldt estuary, *Hydrobiologia*, 366, 1-14, <https://doi.org/10.1023/a:1003164009031>, 1997.

Balke, T., Stock, M., Jensen, K., Bouma, T.J., and Kleyer, M.: A global analysis of the seaward salt marsh extent: The importance of tidal range, *Water Resour. Res.*, 52, 3775-3786, <https://doi.org/10.1002/2015wr018318>, 2016.

Balzter, H., Braun, P.W., and Köhler, W.: Cellular automata models for vegetation dynamics, *Ecol. Model.*, 107, 113-125, [https://doi.org/10.1016/s0304-3800\(97\)00202-0](https://doi.org/10.1016/s0304-3800(97)00202-0), 1998.

Baptist, M.J., Babovic, V., Rodriguez Uthurburu, J., Keijzer, M., Uittenbogaard, R.E., Mynett, A., and Verwey, A.: On inducing equations for vegetation resistance, *J. Hydraul. Res.*, 45, 435-450, <https://doi.org/10.1080/00221686.2007.9521778>, 2007.

Barbier, E.B.: A global strategy for protecting vulnerable coastal populations, *Science*, 345, 1250-1251, <https://doi.org/10.1126/science.1254629>, 2014.

Barbier, E.B., Hacker, S.D., Kennedy, C., Koch, E.W., Stier, A.C., and Silliman, B.R.: The value of estuarine and coastal ecosystem services, *Ecol. Monogr.*, 81, 169-193, <https://doi.org/10.1890/10-1510.1>, 2011.

Baustian, J.J., Mendelssohn, I.A., and Hester, M.W.: Vegetation's importance in regulating surface elevation in a coastal salt marsh facing elevated rates of sea level rise, *Glob. Change Biol.*, 18, 3377-3382, <https://doi.org/10.1111/j.1365-2486.2012.02792.x>, 2012.

Belliard, J.P., Toffolon, M., Carniello, L., and D'Alpaos, A.: An ecogeomorphic model of tidal channel initiation and elaboration in progressive marsh accretional contexts, *J. Geophys. Res.-Earth*, 120, 1040-1064, <https://doi.org/10.1002/2015jf003445>, 2015.

Bertness, M.D. and Ellison, A.M.: Determinants of pattern in a New England salt marsh plant community, *Ecol. Monogr.*, 57, 129-147, <https://doi.org/10.2307/1942621>, 1987.

Best, Ü.S.N., Van der Wegen, M., Dijkstra, J., Willemsen, P.W.J.M., Borsje, B.W., and Roelvink, D.J.A.: Do salt marshes survive sea level rise? Modelling wave action, morphodynamics and vegetation dynamics, *Environ. Modell. Softw.*, 109, 152-166, <https://doi.org/10.1016/j.envsoft.2018.08.004>, 2018.

Bij de Vaate, I., Brückner, M.Z.M., Kleinhans, M.G., and Schwarz, C.: On the impact of salt marsh pioneer species-assemblages on the emergence of intertidal channel networks, *Water Resour. Res.*, 56, e2019WR025942, <https://doi.org/10.1029/2019WR025942>, 2020.

Boerema, A., Geerts, L., Oosterlee, L., Temmerman, S., and Meire, P.: Ecosystem service delivery in restoration projects: the effect of ecological succession on the benefits of tidal marsh restoration, *Ecol. Soc.*, 21, 10, <https://doi.org/10.5751/es-08372-210210>, 2016.

Boesch, D.F. and Turner, R.E.: Dependence of fishery species on salt marshes: The role of food and refuge, *Estuaries*, 7, 460-468, <https://doi.org/10.2307/1351627>, 1984.

Bouma, T.J., Temmerman, S., van Duren, L.A., Martini, E., Vandenbruwaene, W., Callaghan, D.P., Balke, T., Biermans, G., Klaassen, P.C., van Steeg, P., Dekker, F., van de Koppel, J., de Vries, M.B., and Herman, P.M.J.: Organism traits determine the strength of scale-dependent bio-geomorphic feedbacks: A flume study on three intertidal plant species, *Geomorphology*, 180-181, 57-65, <https://doi.org/10.1016/j.geomorph.2012.09.005>, 2013.

Bouma, T.J., van Belzen, J., Balke, T., van Dalen, J., Klaassen, P., Hartog, A.M., Callaghan, D.P., Hu, Z., Stive, M.J.F., Temmerman, S., and Herman, P.M.J.: Short-term mudflat dynamics drive long-term cyclic salt marsh dynamics, *Limnol. Oceanogr.*, 61, 2261-2275, <https://doi.org/10.1002/lno.10374>, 2016.

Breaux, A., Farber, S., and Day, J.: Using natural coastal wetlands systems for wastewater treatment: An economic benefit analysis, *J. Environ. Manage.*, 44, 285-291, <https://doi.org/10.1006/jema.1995.0046>, 1995.

Brückner, M.Z.M., Schwarz, C., Dijk, W.M., Oorschot, M., Douma, H., and Kleinhans, M.G.: Salt marsh establishment and eco-engineering effects in dynamic estuaries determined by species growth and mortality, *J. Geophys. Res.-Earth*, 124, 2962-2986, <https://doi.org/10.1029/2019jf005092>, 2019.

Cao, H., Zhu, Z., Balke, T., Zhang, L., and Bouma, T.J.: Effects of sediment disturbance regimes on *Spartina* seedling establishment: Implications for salt marsh creation and restoration, *Limnol. Oceanogr.*, 63, 647-659, <https://doi.org/10.1002/lno.10657>, 2018.

Chambers, R.M., Osgood, D.T., Bart, D.J., and Montalto, F.: Phragmites australis invasion and expansion in tidal wetlands: Interactions among salinity, sulfide, and hydrology, *Estuaries*, 26, 398-406, <https://doi.org/10.1007/bf02823716>, 2003.

Chang, E.R., Veeneklaas, R.M., Bakker, J.P., Daniels, P., and Esselink, P.: What factors determined restoration success of a salt marsh ten years after de-embankment? *Appl. Veg. Sci.*, 19, 66-77, <https://doi.org/10.1111/avsc.12195>, 2016.

Chen, M.S., Wartel, S., Van Eck, B., and Van Maldegem, D.: Suspended matter in the Scheldt estuary, *Hydrobiologia*, 540, 79-104, <https://doi.org/10.1007/s10750-004-7122-y>, 2005.

Chirol, C., Haigh, I.D., Pontee, N., Thompson, C.E., and Gallop, S.L.: Parametrizing tidal creek morphology in mature saltmarshes using semi-automated extraction from lidar, *Remote Sens. Environ.*, 209, 291-311, <https://doi.org/10.1016/j.rse.2017.11.012>, 2018.

Cox, T., Maris, T., De Vleeschauwer, P., De Mulder, T., Soetaert, K., and Meire, P.: Flood control areas as an opportunity to restore estuarine habitat, *Ecol. Eng.*, 28, 55-63, <https://doi.org/10.1016/j.ecoleng.2006.04.001>, 2006.

Craft, C., Clough, J., Ehman, J., Joye, S., Park, R., Pennings, S., Guo, H., and Machmuller, M.: Forecasting the effects of accelerated sea-level rise on tidal marsh ecosystem services, *Front. Ecol. Environ.*, 7, 73-78, <https://doi.org/10.1890/070219>, 2009.

Dale, J., Burgess, H.M., and Cundy, A.B.: Sedimentation rhythms and hydrodynamics in two engineered environments in an open coast managed realignment site, *Mar. Geol.*, 383, 120-131, <https://doi.org/10.1016/j.margeo.2016.12.001>, 2017.

D'Alpaos, A., Lanzoni, S., Mudd, S.M., and Fagherazzi, S.: Modeling the influence of hydroperiod and vegetation on the cross-sectional formation of tidal channels, *Estuar. Coast. Shelf S.*, 69, 311-324, <https://doi.org/10.1016/j.ecss.2006.05.002>, 2006.

D'Alpaos, A., Lanzoni, S., Marani, M., and Rinaldo, A.: Landscape evolution in tidal embayments: Modeling the interplay of erosion, sedimentation, and vegetation dynamics, *J. Geophys. Res.*, 112, F01008, <https://doi.org/10.1029/2006jf000537>, 2007.

655 Deegan, L.A., Johnson, D.S., Warren, R.S., Peterson, B.J., Fleeger, J.W., Fagherazzi, S., and Wollheim, W.M.: Coastal eutrophication as a driver of salt marsh loss, *Nature*, 490, 388-392, <https://doi.org/10.1038/nature11533>, 2012.

Doody, J.P.: Coastal squeeze and managed realignment in southeast England, does it tell us anything about the future? *Ocean Coast. Manage.*, 79, 34-41, <https://doi.org/10.1016/j.ocecoaman.2012.05.008>, 2013.

Einstein, H.A. and Krone, R.B.: Experiments to determine modes of cohesive sediment transport in salt water, *J. Geophys. Res.*, 660 67, 1451-1461, <https://doi.org/10.1029/jz067i004p01451>, 1962.

Fagherazzi, S., Bortoluzzi, A., Dietrich, W.E., Adami, A., Lanzoni, S., Marani, M., and Rinaldo, A.: Tidal networks 1. Automatic network extraction and preliminary scaling features from digital terrain maps, *Water Resour. Res.*, 35, 3891-3904, <https://doi.org/10.1029/1999wr900236>, 1999.

665 Fagherazzi, S., Kirwan, M.L., Mudd, S.M., Guntenspergen, G.R., Temmerman, S., D'Alpaos, A., van de Koppel, J., Rybczyk, J.M., Reyes, E., Craft, C., and Clough, J.: Numerical models of salt marsh evolution: Ecological, geomorphic, and climatic factors, *Rev. Geophys.*, 50, RG1002, <https://doi.org/10.1029/2011rg000359>, 2012.

Fagherazzi, S., Mariotti, G., Leonardi, N., Canestrelli, A., Nardin, W., and Kearney, W.S.: Salt marsh dynamics in a period of accelerated sea level rise, *J. Geophys. Res.-Earth*, 125, e2019JF005200, <https://doi.org/10.1029/2019jf005200>, 2020.

670 Francalanci, S., Bendoni, M., Rinaldi, M., and Solari, L.: Ecomorphodynamic evolution of salt marshes: Experimental observations of bank retreat processes, *Geomorphology*, 195, 53-65, <https://doi.org/10.1016/j.geomorph.2013.04.026>, 2013.

French, P.W.: Managed realignment – The developing story of a comparatively new approach to soft engineering, *Estuar. Coast. Shelf S.*, 67, 409-423, <https://doi.org/10.1016/j.ecss.2005.11.035>, 2006.

French, C.E., French, J.R., Clifford, N.J., and Watson, C.J.: Sedimentation-erosion dynamics of abandoned reclamations: the role of waves and tides, *Cont. Shelf Res.*, 20, 1711-1733. [https://doi.org/10.1016/s0278-4343\(00\)00044-3](https://doi.org/10.1016/s0278-4343(00)00044-3), 2000.

675 Friess, D.A., Möller, I., Spencer, T., Smith, G.M., Thomson, A.G., and Hill, R.A.: Coastal saltmarsh managed realignment drives rapid breach inlet and external creek evolution, Freiston Shore (UK), *Geomorphology*, 208, 22-33, <https://doi.org/10.1016/j.geomorph.2013.11.010>, 2014.

Gedan, K.B., Silliman, B.R., and Bertness, M.D.: Centuries of human-driven change in salt marsh ecosystems, *Annu. Rev. Mar. Sci.*, 1, 117-141, <https://doi.org/10.1146/annurev.marine.010908.163930>, 2009.

680 Gedan, K.B., Kirwan, M.L., Wolanski, E., Barbier, E.B., and Silliman, B.R.: The present and future role of coastal wetland vegetation in protecting shorelines: answering recent challenges to the paradigm, *Climatic Change*, 106, 7-29, <https://doi.org/10.1007/s10584-010-0003-7>, 2011.

685 Gourgue, O., van Belzen, J., Schwarz, C., Bouma, T.J., van de Koppel, J., and Temmerman, S.: A convolution method to assess subgrid-scale interactions between flow and patchy vegetation in biogeomorphic models, *J. Adv. Model. Earth Sy.*, 13, e2020MS002116, <https://doi.org/10.1029/2020MS002116>, 2021.

Hervouet, J.-M.: *Hydrodynamics of free surface flows: modelling with the finite element method*. Wiley-Blackwell, 2007.

Hinkle, R.L. and Mitsch, W.J.: Salt marsh vegetation recovery at salt hay farm wetland restoration sites on Delaware Bay, *Ecol. Eng.*, 25, 240-251, <https://doi.org/10.1016/j.ecoleng.2005.04.011>, 2005.

690 Hood, W.G.: Differences in tidal channel network geometry between reference marshes and marshes restored by historical dike breaching, *Ecol. Eng.*, 71, 563-573, <https://doi.org/10.1016/j.ecoleng.2014.07.076>, 2014.

Hood, W.G.: Predicting the number, orientation and spacing of dike breaches for tidal marsh restoration, *Ecol. Eng.*, 83, 319-327, <https://doi.org/10.1016/j.ecoleng.2015.07.002>, 2015.

695 Hopkinson, C.S., Morris, J.T., Fagherazzi, S., Wollheim, W.M., and Raymond, P.A.: Lateral marsh edge erosion as a source of sediments for vertical marsh accretion, *J. Geophys. Res.-Biogeo.*, 123, 2444-2465, <https://doi.org/10.1029/2017jg004358>, 2018.

Howes, N.C., FitzGerald, D.M., Hughes, Z.J., Georgiou, I.Y., Kulp, M.A., Miner, M.D., Smith, J.M., and Barras, J.A.: Hurricane-induced failure of low salinity wetlands, *P. Natl. Acad. Sci. USA*, 107, 14014-14019, <https://doi.org/10.1073/pnas.0914582107>, 2010.

700 Hu, Z., van Belzen, J., van der Wal, D., Balke, T., Wang, Z.B., Stive, M., and Bouma, T.J.: Windows of opportunity for salt marsh vegetation establishment on bare tidal flats: The importance of temporal and spatial variability in hydrodynamic forcing, *J. Geophys. Res.-Biogeo.*, 120, 1450-1469, <https://doi.org/10.1002/2014jg002870>, 2015.

Huguet, J.R., Bertin, X., and Arnaud, G.: Managed realignment to mitigate storm-induced flooding: A case study in La Faute-sur-mer, France, *Coast. Eng.*, 134, 168-176, <https://doi.org/10.1016/j.coastaleng.2017.08.010>, 2018.

705 IPCC: *IPCC Special Report on the Ocean and Cryosphere in a Changing Climate*, 2019.

Jongepier, I., Wang, C., Missiaen, T., Soens, T., and Temmerman, S.: Intertidal landscape response time to dike breaching and stepwise re-embankment: A combined historical and geomorphological study, *Geomorphology*, 236, 64-78, <https://doi.org/10.1016/j.geomorph.2015.02.012>, 2015.

Kearney, W.S. and Fagherazzi, S.: Salt marsh vegetation promotes efficient tidal channel networks, *Nat. Commun.*, 7, 12287, <https://doi.org/10.1038/ncomms12287>, 2016.

710 Kirwan, M.L., Guntenspergen, G.R., D'Alpaos, A., Morris, J.T., Mudd, S.M., and Temmerman, S.: Limits on the adaptability of coastal marshes to rising sea level, *Geophys. Res. Lett.*, 37, L23401, <https://doi.org/10.1029/2010gl045489>, 2010.

Kirwan, M.L. and Megonigal, J.P.: Tidal wetland stability in the face of human impacts and sea-level rise, *Nature*, 504, 53-60, <https://doi.org/10.1038/nature12856>, 2013.

715 Kirwan, M.L., Temmerman, S., Skeehan, E.E., Guntenspergen, G.R., and Fagherazzi, S.: Overestimation of marsh vulnerability to sea level rise, *Nat. Clim. Change*, 6, 253-260, <https://doi.org/10.1038/nclimate2909>, 2016.

Lawrence, P.J., Smith, G.R., Sullivan, M.J.P., and Mossman, H.L.: Restored saltmarshes lack the topographic diversity found in natural habitat, *Ecol. Eng.*, 115, 58-66, <https://doi.org/10.1016/j.ecoleng.2018.02.007>, 2018.

Leonardi, N., Ganju, N.K., and Fagherazzi, S.: A linear relationship between wave power and erosion determines salt-marsh resilience to violent storms and hurricanes, *P. Natl. Acad. Sci. USA*, 113, 64-68, <https://doi.org/10.1073/pnas.1510095112>, 2016.

720 Lesser, G.R., Roelvink, J.A., van Kester, J.A.T.M., and Stelling, G.S.: Development and validation of a three-dimensional morphological model, *Coast. Eng.*, 51, 883-915, <https://doi.org/10.1016/j.coastaleng.2004.07.014>, 2004.

Liu, Z., Cui, B., and He, Q.: Shifting paradigms in coastal restoration: Six decades' lessons from China, *Sci. Total Environ.*, 725 566, 205-214, <https://doi.org/10.1016/j.scitotenv.2016.05.049>, 2016.

Liu, Z., Fagherazzi, S., and Cui, B.: Success of coastal wetlands restoration is driven by sediment availability, *Communications Earth and Environment*, 2, 44, <https://doi.org/10.1038/s43247-021-00117-7>, 2021.

Marani, M., Belluco, E., D'Alpaos, A., Defina, A., Lanzoni, S., and Rinaldo, A.: On the drainage density of tidal networks, *Water Resour. Res.*, 39, 1040, <https://doi.org/10.1029/2001wr001051>, 2003.

730 Mariotti, G.: Beyond marsh drowning: The many faces of marsh loss (and gain), *Adv. Water Resour.*, 144, 103710, <https://doi.org/10.1016/j.advwatres.2020.103710>, 2020.

Mariotti, G. and Canestrelli, A.: Long-term morphodynamics of muddy backbarrier basins: Fill in or empty out? *Water Resour. Res.*, 53, 7029-7054, <https://doi.org/10.1002/2017wr020461>, 2017.

735 Mariotti, G., Spivak, A.C., Luk, S.Y., Ceccherini, G., Tyrrell, M., and Gonnea, M.E.: Modeling the spatial dynamics of marsh ponds in New England salt marshes, *Geomorphology*, 365, 107262, <https://doi.org/10.1016/j.geomorph.2020.107262>, 2020.

Maris, T., Cox, T., Temmerman, S., De Vleeschauwer, P., Van Damme, S., De Mulder, T., Van den Bergh, E., and Meire, P.: Tuning the tide: creating ecological conditions for tidal marsh development in a flood control area, *Hydrobiologia*, 588, 31-43, <https://doi.org/10.1007/s10750-007-0650-5>, 2007.

740 McDonald, J.H.: *Handbook of Biological Statistics*, 3rd edition, Sparky House Publishing, Baltimore, Maryland, 2014.

Meire, P., Ysebaert, T., Van Damme, S., Van den Bergh, E., Maris, T., and Struyf, E.: The Scheldt estuary: a description of a changing ecosystem, *Hydrobiologia*, 540, 1-11, <https://doi.org/10.1007/s10750-005-0896-8>, 2005.

Möller, I.: Quantifying saltmarsh vegetation and its effect on wave height dissipation: Results from a UK East coast saltmarsh, *Estuar. Coast. Shelf S.*, 69, 337-351, <https://doi.org/10.1016/j.ecss.2006.05.003>, 2006.

745 Möller, I., Kudella, M., Rupprecht, F., Spencer, T., Paul, M., van Wesenbeeck, B.K., Wolters, G., Jensen, K., Bouma, T.J.,  
Miranda-Lange, M., and Schimmels, S.: Wave attenuation over coastal salt marshes under storm surge conditions, *Nat. Geosci.*, 7, 727-731, <https://doi.org/10.1038/ngeo2251>, 2014.

750 Mossman, H.L., Davy, A.J., and Grant, A.: Does managed coastal realignment create saltmarshes with 'equivalent biological characteristics' to natural reference sites? *J. Appl. Ecol.*, 49, 1446-1456, <https://doi.org/10.1111/j.1365-2664.2012.02198.x>, 2012.

O'Brien, E.L. and Zedler, J.B.: Accelerating the restoration of vegetation in a Southern California salt marsh, *Wetl. Ecol. Manag.*, 14, 269-286, <https://doi.org/10.1007/s11273-005-1480-8>, 2006.

Oosterlee, L., Cox, T.J.S., Vandenbruwaene, W., Maris, T., Temmerman, S., and Meire, P.: Tidal marsh restoration design affects feedbacks between inundation and elevation change, *Estuar. Coast.*, 41, 613-625, <https://doi.org/10.1007/s12237-017-0314-2>, 2018.

755 Oosterlee, L., Cox, T.J.S., Temmerman, S., and Meire, P.: Effects of tidal re-introduction design on sedimentation rates in previously embanked tidal marshes, *Estuar. Coast. Shelf S.*, 244, 106428, <https://doi.org/10.1016/j.ecss.2019.106428>, 2020.

Paramor, O.A.L. and Hughes, R.G.: Effects of the invertebrate infauna on early saltmarsh plant colonisation of managed realignment areas in south-east England, *Mar. Ecol. Prog. Ser.*, 303, 61-71, <https://doi.org/10.3354/meps303061>, 2005.

760 Partheniades, E.: Erosion and deposition of cohesive soils, *J. Hydr. Div.-ASCE*, 91, 105-139, 1965.

Planet Team: Planet application program interface: In space for life on Earth. San Francisco, CA, <https://api.planet.com>, 2017.

Rigon, R., Rodriguez-Iturbe, I., Maritan, A., Giacometti, A., Tarboton, D.G., and Rinaldo, A.: On Hack's Law, Water Resour. Res., 32, 3367-3374, <https://doi.org/10.1029/96wr02397>, 1996.

765 Roelvink, J.A.: Coastal morphodynamic evolution techniques, *Coast. Eng.*, 53, 277-287, <https://doi.org/10.1016/j.coastaleng.2005.10.015>, 2006.

Rogers, K., Kelleway, J.J., Saintilan, N., Megonigal, J.P., Adams, J.B., Holmquist, J.R., Lu, M., Schile-Beers, L., Zawadzki, A., Mazumder, D., and Woodroffe, C.D.: Wetland carbon storage controlled by millennial-scale variation in relative sea-level rise, *Nature*, 567, 91-95, <https://doi.org/10.1038/s41586-019-0951-7>, 2019.

770 Rozas, L.P. and Minello, T.J.: Marsh terracing as a wetland restoration tool for creating fishery habitat, *Wetlands*, 21, 327-341, 2001.

Santín, C., de la Rosa, J.M., Knicker, H., Otero, X.L., Álvarez, M.Á., and González-Vila, F.J.: Effects of reclamation and regeneration processes on organic matter from estuarine soils and sediments, *Org. Geochem.*, 40, 931-941, <https://doi.org/10.1016/j.orggeochem.2009.06.005>, 2009.

775 Schoutens, K., Heuner, M., Minden, V., Ostermann, T.S., Silinski, A., Belliard, J.-P., and Temmerman, S.: How effective are tidal marshes as nature-based shoreline protection throughout seasons? *Limnol. Oceanogr.*, 64, 1750-1762, <https://doi.org/10.1002/lno.11149>, 2019.

Schoutens, K., Heuner, M., Fuchs, E., Minden, V., Schulte-Ostermann, T., Belliard, J.-P., Bouma, T.J., and Temmerman, S.: Nature-based shoreline protection by tidal marsh plants depends on trade-offs between avoidance and attenuation of hydrodynamic forces, *Estuar. Coast. Shelf S.*, 236, 106645, <https://doi.org/10.1016/j.ecss.2020.106645>, 2020.

780 Schuerch, M., Spencer, T., Temmerman, S., Kirwan, M.L., Wolff, C., Lincke, D., McOwen, C.J., Pickering, M.D., Reef, R., Vafeidis, A.T., Hinkel, J., Nicholls, R.J., and Brown, S.: Future response of global coastal wetlands to sea-level rise, *Nature*, 561, 231-234, <https://doi.org/10.1038/s41586-018-0476-5>, 2018.

Schwarz, C., Bouma, T.J., Zhang, L.Q., Temmerman, S., Ysebaert, T., and Herman, P.M.J.: Interactions between plant traits and sediment characteristics influencing species establishment and scale-dependent feedbacks in salt marsh ecosystems, *Geomorphology*, 250, 298-307, <https://doi.org/10.1016/j.geomorph.2015.09.013>, 2015.

785 Schwarz, C., Gourgue, O., van Belzen, J., Zhu, Z., Bouma, T.J., van de Koppel, J., Ruessink, G., Claude, N., and Temmerman, S.: Self-organization of a biogeomorphic landscape controlled by plant life-history traits, *Nat. Geosci.*, 11, 672-677, <https://doi.org/10.1038/s41561-018-0180-y>, 2018.

790 Silliman, B.R., van de Koppel, J., Bertness, M.D., Stanton, L.E., and Mendelsohn, I.A.: Drought, snails, and large-scale die-off of Southern U.S. salt marshes, *Science*, 310, 1803-1806, <https://doi.org/10.1126/science.1118229>, 2005.

Smolders, S., Plancke, Y., Ides, S., Meire, P., and Temmerman, S.: Role of intertidal wetlands for tidal and storm tide attenuation along a confined estuary: a model study, *Nat. Hazard. Earth Sys.*, 15, 1659-1675, <https://doi.org/10.5194/nhess-15-1659-2015>, 2015.

795 Smolders, S., Teles, M.J., Leroy, A., Maximova, T., Meire, P., and Temmerman, S.: Modeling storm surge attenuation by an integrated nature-based and engineered flood defense system in the Scheldt Estuary (Belgium), *Journal of Marine Science and Engineering*, 8, 27, <https://doi.org/10.3390/jmse8010027>, 2020.

Spencer, K.L. and Harvey, G.L.: Understanding system disturbance and ecosystem services in restored saltmarshes: Integrating physical and biogeochemical processes, *Estuar. Coast. Shelf S.*, 106, 23-32, <https://doi.org/10.1016/j.ecss.2012.04.020>, 2012.

800 Spencer, T., Schuerch, M., Nicholls, R.J., Hinkel, J., Lincke, D., Vafeidis, A.T., Reef, R., McFadden, L., and Brown, S.: Global coastal wetland change under sea-level rise and related stresses: The DIVA Wetland Change Model, *Global Planet. Change*, 139, 15-30, <https://doi.org/10.1016/j.gloplacha.2015.12.018>, 2016.

Stark, J., Smolders, S., Meire, P., and Temmerman, S.: Impact of intertidal area characteristics on estuarine tidal hydrodynamics: A modelling study for the Scheldt Estuary, *Estuar. Coast. Shelf S.*, 198, 138-155, <https://doi.org/10.1016/j.ecss.2017.09.004>, 2017.

805 Staver, L.W., Stevenson, J.C., Cornwell, J.C., Nidzieko, N.J., Staver, K.W., Owens, M.S., Logan, L., Kim, C., and Malkin, S.Y.: Tidal marsh restoration at Poplar Island: II. Elevation trends, vegetation development, and carbon dynamics, *Wetlands*, 40, 1687-1701, <https://doi.org/10.1007/s13157-020-01295-4>, 2020.

810 Suir, G.M., Sasser, C.E., DeLaune, R.D., and Murray, E.O.: Comparing carbon accumulation in restored and natural wetland soils of coastal Louisiana, *Int. J. Sediment Res.*, 34, 600-607, <https://doi.org/10.1016/j.ijsrc.2019.05.001>, 2019.

Syvitski, J.P.M., Kettner, A.J., Overeem, I., Hutton, E.W.H., Hannon, M.T., Brakenridge, G.R., Day, J., Vörösmarty, C., Saito, Y., Giosan, L., and Nicholls, R.J.: Sinking deltas due to human activities. *Nat. Geosci.*, 2, 681-686, <https://doi.org/10.1038/ngeo629>, 2009.

815 Temmerman, S., Govers, G., Wartel, S., and Meire, P.: Modelling estuarine variations in tidal marsh sedimentation: response to changing sea level and suspended sediment concentrations, *Mar. Geol.*, 212, 1-19, <https://doi.org/10.1016/j.margeo.2004.10.021>, 2004.

Temmerman, S., Bouma, T.J., Govers, G., and Lauwaet, D.: Flow paths of water and sediment in a tidal marsh: Relations with marsh developmental stage and tidal inundation height, *Estuaries*, 28, 338-352, <https://doi.org/10.1007/bf02693917>, 820 2005.

Temmerman, S., Bouma, T.J., van de Koppel, J., Van der Wal, D., De Vries, M.B., and Herman, P.M.J.: Vegetation causes channel erosion in a tidal landscape, *Geology*, 35, 631-634, <https://doi.org/10.1130/g23502a.1>, 2007.

Temmerman, S., Meire, P., Bouma, T.J., Herman, P.M.J., Ysebaert, T., and De Vriend, H.J.: Ecosystem-based coastal defence in the face of global change, *Nature*, 504, 79-83, <https://doi.org/10.1038/nature12859>, 2013.

825 Tempest, J.A., Harvey, G.L., and Spencer, K.L.: Modified sediments and subsurface hydrology in natural and recreated salt marshes and implications for delivery of ecosystem services, *Hydrol. Process.*, 29, 2346-2357, <https://doi.org/10.1002/hyp.10368>, 2015.

Tian, B., Wu, W., Yang, Z., and Zhou, Y.: Drivers, trends, and potential impacts of long-term coastal reclamation in China from 1985 to 2010, *Estuar. Coast. Shelf S.*, 170, 83-90, <https://doi.org/10.1016/j.ecss.2016.01.006>, 2016.

830 Törnqvist, T.E., Cahoon, D.R., Morris, J.T., and Day, J.W.: Coastal wetland resilience, accelerated sea-level rise, and the importance of timescale, *AGU Advances*, 2, e2020AV000334, <https://doi.org/10.1029/2020av000334>, 2021.

Tucker, G.E., Catani, F., Rinaldo, A., and Bras, R.L.: Statistical analysis of drainage density from digital terrain data, *Geomorphology*, 36, 187-202, [https://doi.org/10.1016/s0169-555x\(00\)00056-8](https://doi.org/10.1016/s0169-555x(00)00056-8), 2001.

Turner, R.K., Burgess, D., Hadley, D., Coombes, E., and Jackson, N.: A cost-benefit appraisal of coastal managed 835 realignment policy, *Global Environ. Chang.*, 17, 397-407, <https://doi.org/10.1016/j.gloenvcha.2007.05.006>, 2007.

Van Damme, S., Struyf, E., Maris, T., Ysebaert, T., Dehairs, F., Tackx, M., Heip, C., and Meire, P.: Spatial and temporal patterns of water quality along the estuarine salinity gradient of the Scheldt estuary (Belgium and The Netherlands): results of an integrated monitoring approach, *Hydrobiologia*, 540, 29-45, <https://doi.org/10.1007/s10750-004-7102-2>, 2005.

Vandenbruwaene, W., Maris, T., Cox, T.J.S., Cahoon, D.R., Meire, P., and Temmerman, S.: Sedimentation and response to 840 sea-level rise of a restored marsh with reduced tidal exchange: Comparison with a natural tidal marsh, *Geomorphology*, 130, 115-126, <https://doi.org/10.1016/j.geomorph.2011.03.004>, 2011a.

Vandenbruwaene, W., Temmerman, S., Bouma, T.J., Klaassen, P.C., de Vries, M.B., Callaghan, D.P., van Steeg, P., Dekker, F., van Duren, L.A., Martini, E., Balke, T., Biermans, G., Schoelynck, J., and Meire, P.: Flow interaction with dynamic vegetation patches: Implications for biogeomorphic evolution of a tidal landscape, *J. Geophys. Res.*, 116, F01008, 845 <https://doi.org/10.1029/2010jf001788>, 2011b.

Vandenbruwaene, W., Bouma, T.J., Meire, P., and Temmerman, S.: Bio-geomorphic effects on tidal channel evolution: impact of vegetation establishment and tidal prism change, *Earth Surf. Proc. Land.*, 38, 122-132, <https://doi.org/10.1002/esp.3265>, 2013.

Vandenbruwaene, W., Schwarz, C., Bouma, T.J., Meire, P., and Temmerman, S.: Landscape-scale flow patterns over a vegetated tidal marsh and an unvegetated tidal flat: Implications for the landform properties of the intertidal floodplain, *Geomorphology*, 231, 40-52, <https://doi.org/10.1016/j.geomorph.2014.11.020>, 2015.

Van Putte, N., Temmerman, S., Verreydt, G., Seuntjens, P., Maris, T., Heyndrickx, M., Boone, M., Joris, I., and Meire, P.: Groundwater dynamics in a restored tidal marsh are limited by historical soil compaction, *Estuar. Coast. Shelf S.*, 244, 106101, <https://doi.org/10.1016/j.ecss.2019.02.006>, 2020.

van Wesenbeeck, B.K., van de Koppel, J., Herman, P.M.J., and Bouma, T.J.: Does scale-dependent feedback explain spatial complexity in salt-marsh ecosystems? *Oikos*, 117, 152-159, <https://doi.org/10.1111/j.2007.0030-1299.16245.x>, 2008.

Wallace, K.J., Callaway, J.C., and Zedler, J.B.: Evolution of tidal creek networks in a high sedimentation environment: A 5-year experiment at Tijuana Estuary, California, *Estuaries*, 28, 795-811, <https://doi.org/10.1007/bf02696010>, 2005.

Waltham, N.J., Alcott, C., Barbeau, M.A., Cebrian, J., Connolly, R.M., Deegan, L.A., Dodds, K., Goodridge Gaines, L.A., Gilby, B.L., Henderson, C.J., McLuckie, C.M., Minello, T.J., Norris, G.S., Ollerhead, J., Pahl, J., Reinhardt, J.F., Rezek, R.J., Simenstad, C.A., Smith, J.A.M., Sparks, E.L., Staver, L.W., Ziegler, S.L., and Weinstein, M.P.: Tidal marsh restoration optimism in a changing climate and urbanizing seascape, *Estuar. Coast.*, 44, 1681-1690, <https://doi.org/10.1007/s12237-020-00875-1>, 2021.

Wang, C. and Temmerman, S.: Does biogeomorphic feedback lead to abrupt shifts between alternative landscape states?: An empirical study on intertidal flats and marshes, *J. Geophys. Res.-Earth*, 118, 229-240, <https://doi.org/10.1029/2012jf002474>, 2013.

Wang, W., Liu, H., Li, Y., and Su, J.: Development and management of land reclamation in China, *Ocean Coast. Manage.*, 102, 415-425, <https://doi.org/10.1016/j.ocecoaman.2014.03.009>, 2014.

Wang, H., Wal, D., Li, X., van Belzen, J., Herman, P.M.J., Hu, Z., Ge, Z., Zhang, L., and Bouma, T.J.: Zooming in and out: Scale dependence of extrinsic and intrinsic factors affecting salt marsh erosion, *J. Geophys. Res.-Earth*, 122, 1455-1470, <https://doi.org/10.1002/2016jf004193>, 2017.

Wang, Z.B., Vandenbruwaene, W., Taal, M., and Winterwerp, H.: Amplification and deformation of tidal wave in the Upper Scheldt Estuary, *Ocean Dynam.*, 69, 829-839, <https://doi.org/10.1007/s10236-019-01281-3>, 2019.

Wang, D., Bai, J., Gu, C., Gao, W., Zhang, C., Gong, Z., and Cui, B.: Scale-dependent biogeomorphic feedbacks control the tidal marsh evolution under *Spartina alterniflora* invasion, *Sci. Total Environ.*, 776, 146495, <https://doi.org/10.1016/j.scitotenv.2021.146495>, 2021.

Webb, E.L., Friess, D.A., Krauss, K.W., Cahoon, D.R., Guntenspergen, G.R., and Phelps, J.: A global standard for monitoring coastal wetland vulnerability to accelerated sea-level rise, *Nat. Clim. Change*, 3, 458-465, <https://doi.org/10.1038/nclimate1756>, 2013.

880 Weinstein, M.P.: Linking restoration ecology and ecological restoration in estuarine landscapes, *Estuar. Coast.*, 30, 365-370, <https://doi.org/10.1007/bf02700179>, 2007.

Weston, N.B.: Declining sediments and rising seas: an unfortunate convergence for tidal wetlands, *Estuar. Coast.*, 37, 1-23, <https://doi.org/10.1007/s12237-013-9654-8>, 2014.

Wiberg, P.L., Fagherazzi, S., and Kirwan, M.L.: Improving predictions of salt marsh evolution through better integration of data and models, *Annu. Rev. Mar. Sci.*, 12, 389-413, <https://doi.org/10.1146/annurev-marine-010419-010610>, 2020.

885 Willemsen, P.W.J.M., Borsje, B.W., Vuik, V., Bouma, T.J., and Hulscher, S.J.M.H.: Field-based decadal wave attenuating capacity of combined tidal flats and salt marshes, *Coast. Eng.*, 156, 103628, <https://doi.org/10.1016/j.coastaleng.2019.103628>, 2020.

Williams, P.B., Orr, M.K., and Garrity, N.J.: Hydraulic geometry: A geomorphic design tool for tidal marsh channel evolution in wetland restoration projects, *Restor. Ecol.*, 10, 577-590, <https://doi.org/10.1046/j.1526-100x.2002.t01-1-02035.x>, 2002.

Winterwerp, J.C., Wang, Z.B., van Braeckel, A., van Holland, G., and Kösters, F.: Man-induced regime shifts in small estuaries – II: a comparison of rivers, *Ocean Dynam.*, 63, 1293-1306, <https://doi.org/10.1007/s10236-013-0663-8>, 2013.

Wolters, M., Garbutt, A., and Bakker, J.P.: Salt-marsh restoration: evaluating the success of de-embankments in north-west 890 Europe, *Biol. Conserv.*, 123, 249-268, <https://doi.org/10.1016/j.biocon.2004.11.013>, 2005.

Yando, E.S., Osland, M.J., Jones, S.F., and Hester, M.W.: Jump-starting coastal wetland restoration: a comparison of marsh and mangrove foundation species, *Restor. Ecol.*, 27, 1145-1154, <https://doi.org/10.1111/rec.12963>, 2019.

Yang, S.L., Luo, X., Temmerman, S., Kirwan, M., Bouma, T., Xu, K., Zhang, S., Fan, J., Shi, B., Yang, H., Wang, Y.P., Shi, X., and Gao, S.: Role of delta-front erosion in sustaining salt marshes under sea-level rise and fluvial sediment decline. 900 *Limnol. Oceanogr.*, 65, 1990-2009, <https://doi.org/10.1002/lo.11432>, 2020.

Zhao, Q., Bai, J., Huang, L., Gu, B., Lu, Q., and Gao, Z.: A review of methodologies and success indicators for coastal wetland restoration, *Ecol. Indic.*, 60, 442-452, <https://doi.org/10.1016/j.ecolind.2015.07.003>, 2016.

Zhu, Z., Vuik, V., Visser, P.J., Soens, T., van Wesenbeeck, B., van de Koppel, J., Jonkman, S.N., Temmerman, S., and Bouma, T.J.: Historic storms and the hidden value of coastal wetlands for nature-based flood defence, *Nature Sustainability*, 905 3, 853-862, <https://doi.org/10.1038/s41893-020-0556-z>, 2020.